Characterization of Catalytic Surfaces by Isotopic-Transient Kinetics during Steady-State Reaction

Schohn L. Shannon and James G. Goodwin, Jr.*

Chemical and Petroleum Engineering Department, University of Pittsburgh, Pittsburgh, Pennsylvania 15261

Received November 17, 1994 (Revised Manuscript Received February 14, 1995)

Contents

I. Introduction

Steady-state isotopic-transient kinetic analysis (SSITKA) is a very useful technique for the kinetic study of heterogeneous catalytic reactions. Initially developed by Happel,[1] Bennett,[2] and Biloen,[3] SSITKA has been used in a number of studies to determine *in situ* kinetic information about the reaction mechanism and the catalyst-surface reaction intermediates. The technique is based upon the detection of isotopic labels in the reactor effluent species versus time following a switch (step change) in the isotopic labeling of one of the reactant species in the reactor feed. In addition to maintaining isothermal and isobaric reaction conditions, the reactant and product concentrations and flow rates remain undisturbed during the step change. Thus, in the absence of isotopic mass effects, steady-state reaction conditions are maintained under isotopic-transient operation. The reaction intermediates present on the catalyst surface do not change, and unlike for other transient techniques,[4-6] analysis of the steady-state kinetic behavior of the catalyst surface is possible. An isotopic-step input is typically used so that the transient behavior of the less-active catalytic sites is included in the kinetic determinations, information which may be lost when using an isotopic-pulse technique. Steady-state kinetic information which has been obtained from SSITKA includes concentrations of different types of adsorbed reaction intermediates, coverages, surface lifetimes, site heterogeneity, activity distributions, and identification of possible mechanisms.

This overview of SSITKA includes discussions of the technique of steady-state isotopic-transient labeling for kinetic study, the mathematical formalisms used in transient analysis, the kinetic parameters which can be obtained, the experimental considerations of the technique, and the reactions to which SSITKA has been applied.

* To whom all correspondence should be addressed.

II. Experimental Measurement

The SSITKA method is based upon the inclusion of one or more stable isotopic labels in a reactant species. A typical SSITKA reaction system is shown in Figure 1. Beginning at steady-state reaction conditions using a particular isotopic label, the inlet feed stream is switched to another feed stream containing a different isotopic labeling of the reactant species. The result is the introduction of a step input of the new isotopic label in the reactant. If the switch is performed quickly and the feed streams are pressure and flow rate balanced prior to the switch, steady-state conditions, in the absence of isotopic mass effects, of the reaction system are maintained. As the reactant progresses through the reactor and reacts on the catalyst surface to form product, the new isotopic label is distributed between reaction product(s) and unreacted reactant as the old isotopic label is replaced by the new isotopic label. The decaying transient response of the old label and the increasing transient response of the new label are monitored at the system outlet by a mass spectrometer to differentiate between the isotopic masses. If the mass spectrometer is operated under minimal fragmentation of the detected effluent species, the transient responses of the isotopic labels specific to different product species can be determined. A gas chromatograph is usually used to calibrate the mass spectrometer detection of the reactant and product concentrations.

Figure 2 presents the typical transient responses, also termed relaxation curves, of a differential-bed plug-flow reactor (PFR) following a step change in the isotopic labeling of reactant R, R ⇒ *R, which subsequently appears in product P as P ⇒ *P. In Figure 2, the transient response to a step input of the new isotopic label is designated as the $F_m^{*P}(t)$ step-input response of the product (the subscript m indicates a measured response). The step-input response is a statistical distribution representing the probability that an isotopic label remains adsorbed on the catalyst surface or appears in the effluent stream with time. It has become common in SSITKA to use the step-decay response of the old isotopic label (the label prior to the switch), designated by $F_m^{P}(t)$ in Figure 2, in order to follow the isotopic transient. The

0009-2665/95/0795-0677$15.50/0

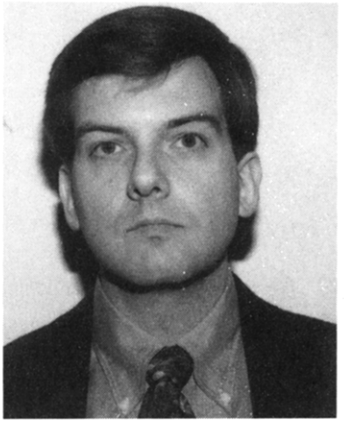

Schohn L. Shannon is president of GS Scientific, Inc. a recently founded research and technological development company. He received his B.S. (BioChem) from the Pennsylvania State University in 1981 and his M.S. (ChE) from the University of Pittsburgh in 1986. Following his M.S., he worked as a research associate at the University of Pittsburgh and as a product engineer at Altamira Instruments, Inc., eventually becoming the manager of R&D, where he worked on the design and manufacture of catalyst-characterization and reactor systems. He returned to the University of Pittsburgh in 1992 to pursue thesis work on modeling methods for steady-state isotopic transient kinetic analysis. His areas of interest include reactor design, reaction kinetic analysis, process design, and mathematical modeling.

James G. Goodwin, Jr. is a William Kepler Whiteford Professor of Chemical Engineering and the Director of the International Technology Center at the University of Pittsburgh. He received a B.S. (ChE) from Clemson University in 1967, an M.S. (ChE) from the Georgia Institute of Technology in 1969, and a Ph.D. (ChE) from the University of Michigan in 1976. Between his M.S. and Ph.D., he served in the Peace Corps. Following his Ph.D., he was an assistant professor at the University of South Carolina and a U.S.–France exchange scientist at the Institut de Recherches sur Catalyse in Villeurbanne, France, before joining the Chemical and Petroleum Engineering Department at the University of Pittsburgh in 1979. He also serves as a consultant to industry. He has widely published, presented, and patented from his research involving heterogeneous catalysis including characterization of supported metal catalysts, modification of catalyst properties by chemical promoters, synthesis of hydrocarbons and oxygenates from CO and H_2, and oxidation of hydrocarbons. His work within the last 8 years has included extensive use of steady-state isotopic-transient kinetic analysis in the study of heterogeneous catalysts.

step-decay response can always be obtained from the step-input response using the relationship:

$$F_m^P(t) = 1 - F_m^{*P}(t) \quad (1)$$

In addition to the isotopic-tracer transient responses, an inert-tracer transient response, $F_m^I(t)$, is also indicated in Figure 2. An inert tracer is used in SSITKA for determination of the gas-phase holdup

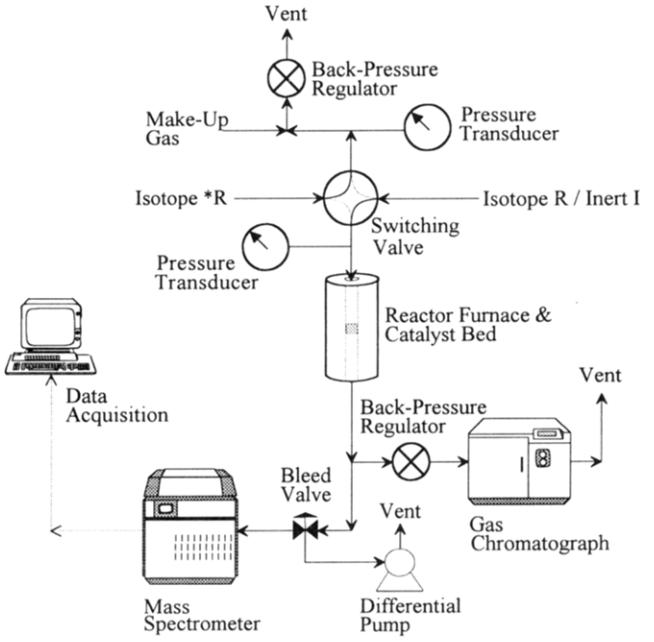

Figure 1. Typical reaction system for steady-state isotopic-transient (SSITKA) experimentation.

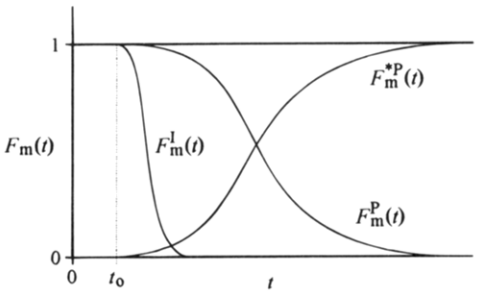

Figure 2. Typical normalized isotopic-transient responses in product species P following an isotopic switch in reactant, R ⟹ *R, which appears in the product as P ⟹ *P. An inert tracer, I, is simultaneously introduced to determine the gas-phase holdup of the reactor system.

for the reactor system and is often introduced by simultaneously including a small concentration of inert in either of the isotopic-tracer feed streams during the step change. The initial time of the transient experiment, t_o, is typically taken as the beginning of the inert-tracer transient response, and all other transient response times are referenced relative to time t_o of the inert-tracer transient response.

III. SSITKA Reaction Parameter Determinations

A. General Parameters—Surface-Intermediate Abundancy and Residence Time

Consider a *reversible* steady-state heterogeneous catalytic reaction:

$$\text{R(g)} + \text{other reactants} \rightleftarrows \text{A intermediates(ads)} \rightleftarrows \text{P(g)} + \text{other products} \quad (2)$$

where reactant species R generates product species P via adsorbed intermediate species A. When the reaction is operated under steady-state conditions, the amounts of R, P, and A, as well as any other

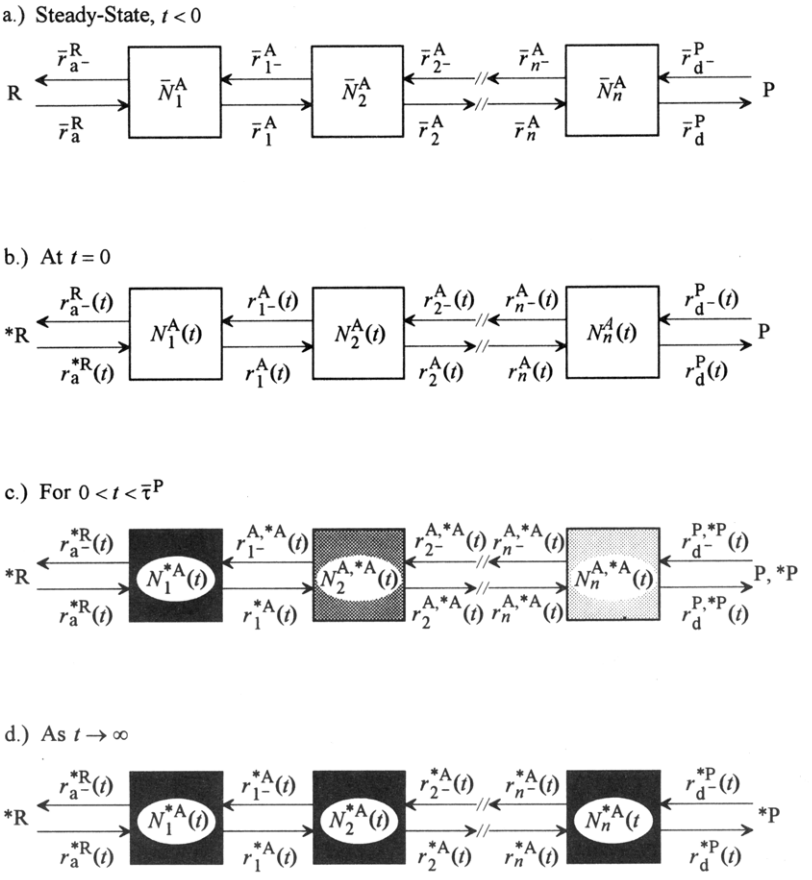

Figure 3. Catalyst–surface model showing the isotopic distribution between n pools in series following an isotopic switch, R ⟹ *R, at the reaction volume inlet.

reactant and product species entering and exiting the reaction pathway, remain constant.

In SSITKA, it is common to consider the catalyst surface to be composed of a system of interconnected pools, also termed compartments,[7] where each pool represents a homogeneous or well-mixed subsystem within the reaction pathway. A separate pool is assumed to exist for each unique adsorbed reaction-intermediate species or type of catalytically active site. It is assumed that there is essentially no mixing or holdup time associated with each pool or within the reaction pathway except for the residence time of a reaction-intermediate species adsorbed on the catalyst surface. Figure 3a presents this concept where an n number of intermediate pools in series represents the steady-state reaction pathway. In Figure 3a, $\bar{N}_i^A$ is the steady-state abundance of the number of atoms of the isotope in each individual ith pool ($i = 1, 2, ..., n$) where the overbar, "–", indicates a steady-state condition. Although not a requirement, a simplification is that only one atom of the isotope is present in each reactant species R, product species P, and intermediate species A. If this case holds, then $\bar{N}_i^A$ is also the steady-state abundance of intermediate species A in the ith pool. Additionally in Figure 3a, $\bar{r}_a^R$ and $\bar{r}_{a^-}^R$ are the respective steady-state adsorption and desorption rates of reactant species R, $\bar{r}_d^P$ and $\bar{r}_{d^-}^P$ are the respective steady-state desorption and readsorption rates of product species P, $\bar{r}_{i^{(-)}}^A$ is the steady-state transfer rate between pools of intermediate species A, and the "–" subscript indicates a reverse pathway. In nondynamic steady-state kinetic studies, the overall reaction rate, $\bar{r}^P$, is typically determined and in this model is equivalent to the difference in the product generation rate and readsorption rate, $\bar{r}^P = \bar{r}_d^P - \bar{r}_{d^-}^P$, for the nth pool. Likewise, the overall steady-state input rate to the reaction, $\bar{r}^R$, for the reactant can be written as $\bar{r}^R = \bar{r}_a^R - \bar{r}_{a^-}^R$. At steady state, $\bar{r}^R = \bar{r}_i^A - \bar{r}_{i^-}^A = \bar{r}^P$.

Now consider that an instantaneous and complete switch occurs at time, $t = 0$, in the isotopic labeling of species R, R ⟹ *R, at the inlet of the reaction volume as indicated in Figure 3b by *R. The new isotopic label in reactant species R progresses along the reaction pathway via reaction intermediates A, resulting in a transient condition in the isotopic labeling for product species P, P ⟹ *P. Ultimately, all of the old isotopic label is displaced by the new isotopic label as indicated in Figure 3d. The distribution of the isotopic labels is dependent upon the steady-state transfer rates, $\bar{r}_{i^{(-)}}^A$, between pools, and the isotopic-transient responses of product-species P are obtained as an increasing, $r^{*P}(t)$, and a decreasing, $r^P(t)$, the rates of formation of product with respective isotopic labels, where $\bar{r}^P = r^P(t) + r^{*P}(t)$.

While the isotopic switch may also result in a transient condition in the isotopic labeling of reactant species R due to adsorption and desorption, the isotopic-transient response for species P can be readily attributed to a residence time on the catalyst surface during reaction. Therefore, it is typical in SSITKA to be most interested in the isotopic-transient response of a product species. SSITKA can be used to investigate various reaction systems using

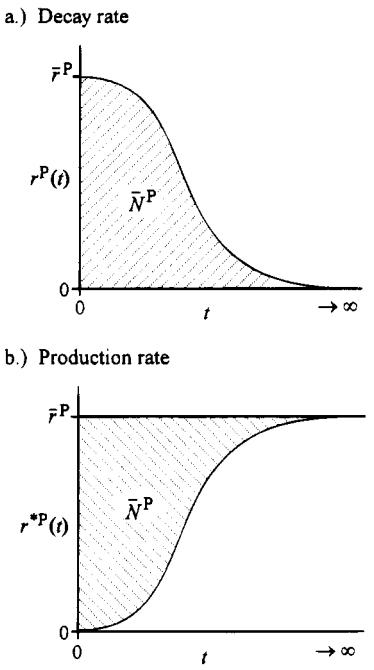

Figure 4. Typical steady-state isotopic transient rate responses showing the surface-intermediate abundance, $\bar{N}^P$, relation to the transients. The responses have been corrected for gas-phase holdup.

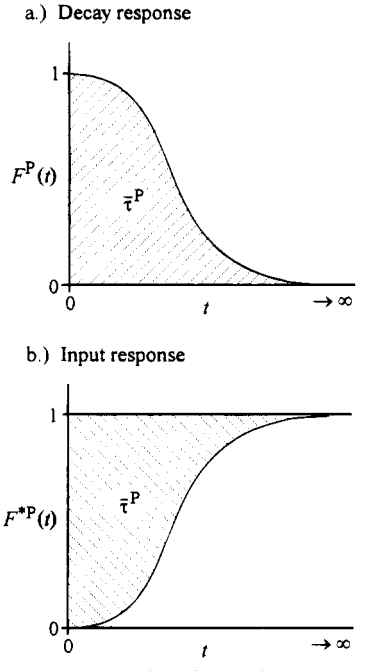

Figure 5. Typical normalized steady-state isotopic transient responses showing the overall mean surface-residence time, $\bar{\tau}^P$, relation to the transients. The responses have been corrected for gas-phase holdup.

other isotopic-labeling stoichiometries, multiple-isotopic labels, multiple isotopically labeled product species, and/or the reactant isotopic-transient response provided one understands where assumptions must be made and the limitations that they imply.

The product species P transient rates can be written in terms of fractional amounts of the steady-state reaction rates, $\bar{r}^P$, as[8]

$$r^P(t) = \bar{r}^P\left(\frac{r^P(t)}{\bar{r}^P}\right) \tag{3}$$

and

$$r^{*P}(t) = \bar{r}^P\left(\frac{r^{*P}(t)}{\bar{r}^P}\right) \tag{4}$$

The resulting isotopic-transient decay and production rates are notionally presented in Figure 4, parts a and b. Following the isotopic switch, the total effluent amount of the old isotopic label in product species P from $t = 0$ (Figure 3b) to $t \to \infty$ (Figure 3d) is equivalent to the total steady-state amount of intermediate species, $\bar{N}^P$, present on the catalyst surface that leads to product species P. Thus, in this model, $\bar{N}^P = \bar{N}_1^A + \bar{N}_2^A + \ldots + \bar{N}_n^A$, which can be obtained from integration of either the isotopic-transient decay (or production) rates of product species P (or *P)

$$\bar{N}^P = \int_0^\infty r^P(t)\,dt = \int_0^\infty [\bar{r}^P - r^{*P}(t)]\,dt \tag{5}$$

This quantity is equivalent to the crosshatched area in either part a or b of Figure 4. Although the series model of Figure 3 has been used to visualize the process, eq 5 is applicable *regardless* of the underlying kinetic model, and SSITKA permits absolute determination of the amount of the most active reaction intermediates leading to a particular product species at steady state. When there is reversible adsorption of the isotopically labeled reactant ($\bar{r}^R_{a-} \neq 0$ in Figure 3a) and/or a reaction pathway leads to multiple product species, $\bar{N}^P$ would represent only the amount of reactive surface intermediates leading to product species P and would only be a fraction of the total adsorbed species. It should be noted that the total amount of adsorbed intermediates, $\bar{N}^P$, is the most general and accurate parameter which is obtained from SSITKA. No assumptions concerning the underlying kinetics or mechanism—i.e., order of the reaction, irreversibility of the reaction, or makeup of the reaction pathway—are required.

Another general parameter which is obtainable in SSITKA is the overall mean surface-residence time or surface lifetime, $\bar{\tau}^P$, of the adsorbed intermediates on the catalyst surface. This mean surface-residence time, also termed the relaxation time, is obtained from the normalized distributions of the decay or production rates of the isotopic transients defined as the step-decay transient response

$$F^P(t) = \frac{r^P(t)}{\bar{r}^P} \tag{6}$$

and the step-input transient response

$$F^{*P}(t) = \frac{r^{*P}(t)}{\bar{r}^P} \tag{7}$$

Normalized transient responses are notionally presented in Figure 5, parts a and b. It can be shown that integration of the normalized step-decay or step-input response *always* yields the overall mean surface-residence time,[9] $\bar{\tau}^P$, of all of the adsorbed surface

intermediates which lead to product species P, or

$$\bar{\tau}^{P} = \int_0^\infty F^{P}(t)\,dt = \int_0^\infty [1 - F^{*P}(t)]\,dt \qquad (8)$$

This quantity is equivalent to the crosshatched area indicated in either part a or b in Figure 5. Like $\bar{N}^{P}$, SSITKA permits determination of the overall mean surface-residence time, $\bar{\tau}^{P}$, of the reaction intermediates at steady state leading to a particular product species *regardless* of the underlying kinetic model, i.e., the reaction rate expression or the reaction pathway. However, this mean surface-residence time is more subjective in its interpretation than the amount of adsorbed intermediate species, especially in the presence of reversible reaction pathways.

Rearranging eq 6, $r^{P}(t) = \bar{r}^{P}F^{P}(t)$, substituting this result into eq 5, and using the integral relation of eq 8 yields

$$\bar{N}^{P} = \int_0^\infty r^{P}(t)\,dt = \bar{r}^{P}\int_0^\infty F^{P}(t)\,dt = \bar{r}^{P}\bar{\tau}^{P} \qquad (9)$$

and rearranging eq 9 yields

$$\bar{r}^{P} = \bar{N}^{P}/\bar{\tau}^{P} \qquad (10)$$

Equation 10 is the general relation for the overall reaction rate at steady state and is also valid *regardless* of the underlying kinetics or mechanism. For non dynamic or global steady-state kinetic experiments, only the overall reaction rate, $\bar{r}^{P}$, is determinable. However, as indicated by eqs 5 and 8, SSITKA permits *separate* measurement of the abundance of surface intermediates which lead to a particular product, $\bar{N}^{P}$, and the overall mean residence time, $\bar{\tau}^{P}$, of those intermediates on the catalyst surface, something which cannot be accomplished by other global steady-state reaction methods where the determined reaction rate is the quotient of these two terms as expressed by eq 10.

While $\bar{N}^{P}$ and $\bar{\tau}^{P}$ are the most general parameters, additional kinetic parameters which can be determined from SSITKA are based upon, and thus specific to, assumptions and mechanistic models for the catalyst-surface reaction. These kinetic parameters are discussed in the following sections.

B. Specific Parameters—Irreversible Catalyst-Surface Models

1. Single Pool—Irreversible Adsorption and Reaction

Consider an *irreversible reaction*

$$R(g) \rightarrow A \text{ intermediates(ads)} \rightarrow P(g) \qquad (11)$$

occurring at a single type of catalytic site (a homogeneous catalytic surface). The reaction pathway can be represented as a *single pool* of adsorbed reaction intermediates as indicated in Figure 6. Expressing

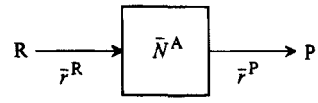

Figure 6. Catalyst-surface single-pool model for irreversible reaction.

an un-steady-state material balance for the irreversible-reaction pathway in the form

$$\text{intermediate accumulation rate} = \text{reactant inlet rate} - \text{product outlet rate} \qquad (12)$$

yields, for the step decay

$$\frac{d}{dt}N^{A}(t) = r^{R}(t) - r^{P}(t) \qquad (13)$$

Dividing both sides of eq 13 by the constant, $\bar{N}^{A}$, yields

$$\frac{d}{dt}\left[\frac{N^{A}(t)}{\bar{N}^{A}}\right] = \frac{r^{R}(t)}{\bar{N}^{A}} - \frac{r^{P}(t)}{\bar{N}^{A}} \qquad (14)$$

The bracketed term in eq 14 is equivalent to the normalized transient response which can be written as $F^{A}(t) = N^{A}(t)/\bar{N}^{A}$. The transient rates can be defined in terms of fractional amounts of their steady-state rates (i.e., $r^{P}(t) = \bar{r}^{P}[r^{P}(t)/\bar{r}^{P}]$). Thus, the respective normalized transient responses can be incorporated into this equation (i.e., $F^{P}(t) = r^{P}(t)/\bar{r}^{P}$). Substituting these quantities into eq 14 yields

$$\frac{d}{dt}F^{A}(t) = \frac{\bar{r}^{R}}{\bar{N}^{A}}F^{R}(t) - \frac{\bar{r}^{P}}{\bar{N}^{A}}F^{P}(t) \qquad (15)$$

For this model, $\bar{r}^{P} = \bar{r}^{R}$, and the mean surface-residence time, $\bar{\tau}^{A}$, is defined as

$$\bar{\tau}^{A} = \left\{\frac{\bar{r}^{R}}{\bar{N}^{A}}\right\}^{-1} = \left\{\frac{\bar{r}^{P}}{\bar{N}^{A}}\right\}^{-1} \qquad (16)$$

Recognizing that in terms of the transient responses for this model, $F^{P}(t) = F^{A}(t)$, eq 15 can be rewritten, using eq 16, as

$$\frac{d}{dt}F^{P}(t) = \{\bar{\tau}^{A}\}^{-1}F^{R}(t) - \{\bar{\tau}^{A}\}^{-1}F^{P}(t) \qquad (17)$$

For a step removal of isotopically labeled R, $F^{R}(t) = 0$ for $t \geq 0$, and integrating eq 17 with the initial boundary condition, $F^{P}(t) = 1$ at $t = 0$, yields

$$F^{P}(t) = \exp(-t/\bar{\tau}^{A}) \qquad (18)$$

Integration of the product transient response, eq 18, yields the overall mean surface-residence time

$$\bar{\tau}^{P} = \int_0^\infty F^{P}(t)\,dt = \bar{\tau}^{A} \qquad (19)$$

Assuming a *pseudo-first-order* rate expression, $\bar{r}^{P} = k\bar{N}^{A}$, where k is the reactivity (the first-order rate constant), then $k = \bar{N}^{A}/\bar{r}^{P}$. Comparing this value for k with the results of eqs 16 and 19 indicates that the pseudo-first-order rate constant is equal to the

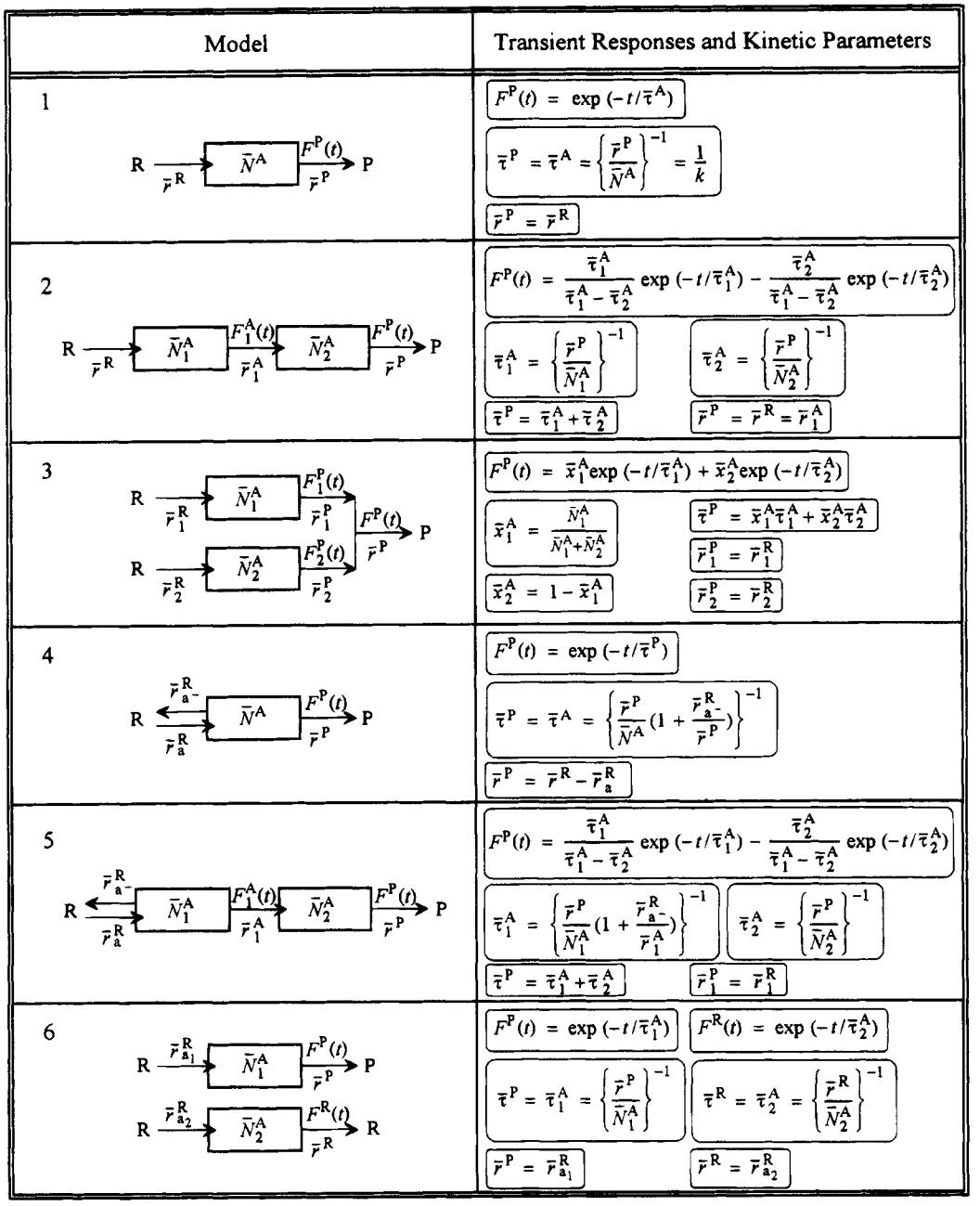

Figure 7. Catalyst-surface mechanistic models, transient responses, and kinetic parameters.

reciprocal of the overall mean surface-residence time, or

$$k = 1/\bar{\tau}^{P} \tag{20}$$

The pseudo-first-order assumption for the overall reaction is somewhat specious, except for those reaction mechanisms which are determined to be true first order. However, while k may also contain the dependence of the rate on the fractional surface coverage of other reactants, the pseudo-first-order reaction model is useful for quantitative comparison of catalytic pathways.[3] The parametric results for the single-intermediate pool with irreversible reaction (model 1), as well as other catalyst-surface models to be discussed, are summarized in Figure 7.

A parameter often used in the comparison of catalytic activity is the turnover frequency, $\overline{\mathrm{TOF}}^{P}$ or turnover number,[10] defined as the generation rate of product species P *per catalyst-surface active site*. The turnover frequency, steady-state reaction rate, $\bar{r}^{P}$, and pseudo-first-order reaction rate can be related by

$$\overline{\mathrm{TOF}}^{P} = \frac{\bar{r}^{P}}{\bar{N}_c} = \frac{\bar{N}^{P}}{\bar{N}_c} k = k\bar{\theta}_c^{P} = \frac{1}{\bar{\tau}^{P}}\bar{\theta}_c^{P} \tag{21}$$

where $\bar{\theta}_c^{P}$ is the fractional coverage in catalyst-surface intermediates, $\bar{\theta}_c^{P} = \bar{N}^{P}/\bar{N}_c$, and $\bar{N}_c$ is the total abundance of catalyst-surface active sites.[3,11] The determination of the $\overline{\mathrm{TOF}}^{P}$ requires a separate measurement of the total number of surface active sites, $\bar{N}_c$, which is often obtained by chemisorption methods. However, this measured $\bar{N}_c$ is often not the true number of active sites for reaction. In contrast, SSITKA permits a direct and separate measurement

of the abundance of surface intermediates, $\bar{N}^P$, and the reactivity, $k = 1/\bar{\tau}^P$, during the reaction at steady state. Consequently, the reactivity, k, determined by SSITKA, assuming first-order reaction, is a more accurate measure of the *absolute* turnover frequency.

2. Pools in Series—Irreversible Adsorption, Intermediate Pathways, and Reaction

The previous material-balance method can be extended to a *serial-pool model* for n number of pools, and the transient response is given by[73]

$$F^P(t) = \sum_{i=1}^{n} \frac{(\bar{\tau}_i^A)^{n-1}}{\prod_{j=1,j\neq i}^{n} (\bar{\tau}_i^A - \bar{\tau}_j^A)} \exp(-t/\bar{\tau}_i^A) \qquad n = 1, 2, 3, \ldots \quad (22)$$

Integration of the product transient response provides the overall mean surface-residence time

$$\bar{\tau}^P = \bar{\tau}_1^A = \bar{\tau}_2^A + \ldots + \bar{\tau}_n^A = \sum_{i=1}^{n} \bar{\tau}_i^A \quad (23)$$

where the individual time constant of each intermediate pool is given by

$$\bar{\tau}_i^A = \{\bar{r}_i^A/\bar{N}_i^A\}^{-1} \quad (24)$$

The parametric results for two pools in series (model 2) is shown in Figure 7. The overall mean surface-residence time of the isotope leading to product P, $\bar{\tau}^P$, is the sum of the time constants for each pool. Since the integration is not able to provide a unique identification of the individual time constants attributable to each pool, other analytical techniques must be employed in order to obtain this information. One method is to use an iterative curve fit of the experimental transient response (corrected for gas-phase holdup) to determine $\bar{\tau}_1^A$ and $\bar{\tau}_2^A$.[12]

3. Pools in Parallel—Irreversible Adsorption and Reaction

A heterogeneous catalyst surface may be characterized by multiple active sites acting in parallel. Each type of site can be represented by a pool with distinct adsorbed surface intermediates.[12] Following a similar derivation as that used for the single-pool model, the transient response for n *parallel pools* with *irreversible reaction* is given by

$$F^P(t) = \sum_{i=1}^{n} \bar{x}_i^A \exp(-t/\bar{\tau}_i^A) \quad (25)$$

where $\bar{x}_i^A$ is the steady-state fractional amount of the surface intermediates in the ith pool

$$\bar{x}_i^A = \frac{\bar{N}_i^A}{\sum_{j=1}^{n} \bar{N}_j^A} \qquad i = 1, 2, \ldots, n \quad (26)$$

Integration of the product transient response yields the overall mean surface-residence time

$$\bar{\tau}^P = \int_0^\infty F^P(t)\, dt = \sum_{i=1}^{n} \bar{x}_i^A \bar{\tau}_i^A \quad (27)$$

where the individual time constant of each intermediate pool is given by

$$\bar{\tau}_i^A = \left\{\frac{\bar{r}_i^P}{\bar{N}_i^A}\right\}^{-1} \quad (28)$$

The parametric results for two parallel pools with irreversible reaction (model 3) is shown in Figure 7. Since the analysis is not able to provide a unique identification of the individual time constants attributable to each pool, other techniques must be employed to separately determine their values. One method uses partial isotopic exchange which is discussed in a subsequent section.

C. Specific Parameters—Reversible Processes

1. Single Pool and Pools in Series—Reversible Adsorption

Consider an *irreversible reaction*,

$$R(g) \rightleftarrows A \text{ intermediates(ads)} \rightarrow P(g) \quad (29)$$

but occurring with *reversible adsorption* of reactant at a *single pool* (model 4 in Figure 7). Expressing a material balance for the reversible pathway in the form of eq 12 and using a similar derivation as used for a single pool with irreversible reaction yields the product transient response

$$F^P(t) = \exp(-t/\bar{\tau}_i^A) \quad (30)$$

Integration of the product transient response yields the overall mean surface-residence time

$$\bar{\tau}^P = \int_0^\infty F^P(t)\, dt = \bar{\tau}^A = \frac{\bar{r}^P}{\bar{N}^A}\left\{1 + \frac{\bar{r}_{a^-}^R}{\bar{r}^P+}\right\}^{-1} \quad (31)$$

If one can assume that the reaction is *pseudo-first order*, then $\bar{r}^P = k\bar{N}^A$ and $k = \bar{r}^P/\bar{N}^A$, thus

$$k = \frac{1}{\bar{\tau}^P}\left(\frac{\bar{r}^P}{\bar{r}^P + \bar{r}_{a^-}^R}\right) \quad (32)$$

If $\bar{r}_{a^-}^R$ can be determined, an exact value for k can be determined. Unfortunately, this rate is difficult to determine. If k is estimated using $1/\bar{\tau}^P$

$$\left[k_{est} = \frac{1}{\bar{\tau}^P}\right] > \left[k = \frac{1}{\bar{\tau}^P}\left(\frac{\bar{r}^P}{\bar{r}^P + \bar{r}_{a^-}^R}\right)\right] \quad (33)$$

then the value determined for k, k_{est}, is the *maximum value* possible. Obviously, as the desorption of reactant R becomes less significant ($\bar{r}_{a^-}^R \ll \bar{r}^P$), k approaches $1/\bar{\tau}^P$.

The previous material-balance method can be readily extended to n number of pools in series. The parametric results for a two-serial-pool model (model

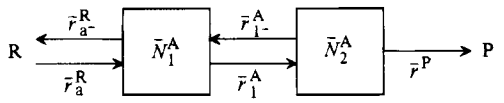

Figure 8. Catalyst-surface two-serial-pool model for irreversible reaction with a reversible reaction-intermediate step and reversible adsorption of reactant.

5) with *reversible adsorption* and *irreversible reaction* are summarized in Figure 7.

2. Pools in Series—Reversible Intermediate Pathways

For a pools-in-series model involving *reversible reaction-intermediate pathways* with *irreversible reaction*, the previous material-balance method yields for a two-pool model (Figure 8) in convenient matrix form[7,8]

$$\frac{\mathrm{d}}{\mathrm{d}t}\begin{bmatrix}F_1^A(t)\\ F^P(t)\end{bmatrix} = \begin{bmatrix} -\left\{\frac{\bar{r}_1^A}{\bar{N}_q^A} + \frac{\bar{r}_{a^-}^R}{\bar{N}_1^A}\right\} & \left\{\frac{\bar{r}_{a^-}^R}{\bar{N}_1^A}\right\} \\ \left\{\frac{\bar{r}_1^A}{\bar{N}_2^A}\right\} & -\left\{\frac{\bar{r}^P}{\bar{N}_2^A} + \frac{\bar{r}_{1^-}^A}{\bar{N}_2^A}\right\} \end{bmatrix}\begin{bmatrix}F_1^A(t)\\ F^P(t)\end{bmatrix} \tag{34}$$

The material balance can be extended to multiple pools in series where each pool requires an additional material-balance equation.

In order to obtain the underlying rate parameters from the transient responses, eq 34 requires solution. Unfortunately, the material balances and their boundary conditions become quite complicated for even simple reaction systems, and attempts at solution often result in analytical impasses. The problem of analytical solution becomes acute in the determination of product transient responses whenever a reversible reaction-intermediate pathway or overall reversible reaction is involved. Consequently, quantitative modeling in SSITKA is currently limited to simpler irreversible-kinetic models. Due to the inherent linearity of the isotopic-tracing method,[8] qualitative analyses using Laplace transforms and transfer functions have been developed to investigate whether it is possible to uniquely identify the rate parameters or determine the difference between proposed surface models without obtaining an analytical solution.[13,14]

3. Intermediate Pools in Parallel—Reversible Adsorption

The transient response for n *parallel pools* with *reversible adsorption* and *irreversible reaction* is similar to the n-parallel-pool irreversible-reaction model, except that the transient response is written in terms of the fractional amounts of the product

$$F^P(t) = \sum_{i=1}^{n} \bar{x}_i^P \exp(-t/\bar{\tau}_i^A) \tag{35}$$

which are given by

$$\bar{x}_i^P = \frac{\bar{N}_i^P}{\sum_{j=1}^{n} \bar{N}_j^P} \qquad i = 1, 2, ..., n \tag{36}$$

The time constant for each pool is given by

$$\bar{\tau}_i^A = \left\{\frac{\bar{r}_i^P}{\bar{N}_i^A}\left(1 + \frac{\bar{r}_{a_i^-}^R}{\bar{r}_i^P}\right)\right\}^{-1} \tag{37}$$

Integration of the product transient response yields the overall mean surface-residence time

$$\bar{\tau}^P = \int_0^\infty F^P(t)\,\mathrm{d}t = \sum_{i=1}^{n} \bar{x}_i^P \bar{\tau}_i^A \tag{38}$$

D. Specific Parameters—Reversible Reaction

The presence of reversible reaction, such as in ammonia synthesis where the NH_3 is in equilibrium with the catalyst surface, presents difficulties in the interpretation of the transient responses.[15] The previous model derivations have excluded reversible reactions because of the inability to be able to obtain analytical solutions for the product transient response based upon catalyst-surface modeling. This difficulty is similar to that encountered when dealing with reversible reaction-intermediate pathways. However, a numerical method using nonlinear least-squares regression has been recently developed for determination of kinetic parameters based upon catalyst−surface models involving reversibility.[93] It should be noted that the presence of reversibility does not prevent determination of the general parameters, $\bar{N}^P$ and $\bar{\tau}^P$, using SSITKA but does lead to increased complexities in the interpretation of these parameters.

E. Surface or Intermediate Heterogeneity

If it can be assumed that a reaction is pseudo-first order, then the relative heterogeneity of the catalyst surface can be determined by the logarithmic behavior of the isotopic transient. Figure 9 presents the semilogarithmic plot for both the single-pool (homogeneous) and parallel-pool (heterogeneous) models. The presence of curvature in the plot is indicative of surface heterogeneity (i.e., multiple pools in parallel).[15]

If the parallel-pool model for pseudo-first-order irreversible reaction is extended to an infinite number of pools in parallel, the heterogeneity of the

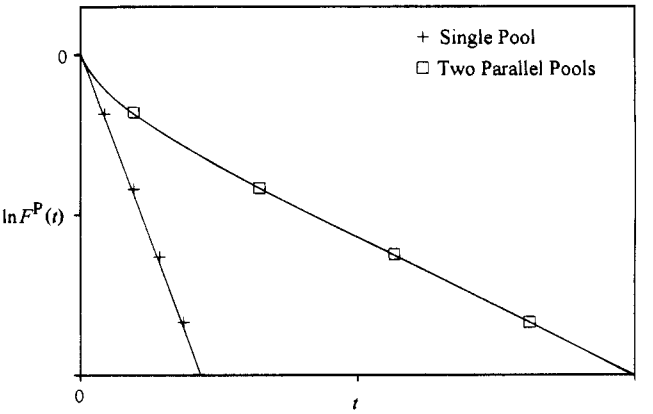

Figure 9. Semilogarithmic plot contrasting homogeneous and heterogeneous catalytic-surface isotopic-transient responses.[15]

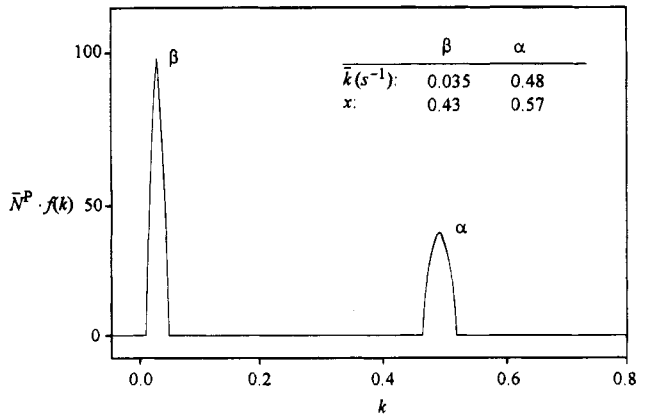

Figure 10. Reactivity distribution of methanation over a Ru/SiO_2 catalyst.[17]

catalytic surface can be characterized by a reactivity distribution, $f(k)$. Substituting eqs 6 and 10 into eq 25, where $k = 1/\bar{\tau}^A$, yields[16]

$$r^P(t) = \bar{N}^P \sum_{i=1}^{n} \bar{x}_i^A k \exp(-kt) \qquad (39)$$

If $n \to \infty$, this can be rewritten in integral form as[16,17]

$$r^P(t) = \bar{N}^P \int_0^\infty k \exp(-kt) f(k)\, dk \qquad (40)$$

The determination of $f(k)$ from eq 40 requires a numerical deconvolution technique. To date, a parametric[18] and two nonparametric methods[16,17] have been developed for this deconvolution. The advantage of the nonparametric techniques is that no assumption about the form of $f(k)$ is required. Both nonparametric methods require dynamic numerical smoothing since deconvolution is susceptible to noise or error in the data which results in extreme numerical-deconvolution oscillations. One nonparametric method[16] utilizes an inverse-Laplace-transform technique since the form of eq 40 is equivalent to the Laplace transform [kernel = $\exp(-kt)$] of the function $k f(k)$. A second nonparametric method[17] recognizes that the form of eq 40 is also a Fredholm integral [kernel = $k \exp(-kt)$] and utilizes a nonlinear least-squares curve fit of the transient response data based upon the Tikhonov regularization which is more precise but computationally demanding. Figure 10 presents a reactivity distribution obtained by the Tikonov–Fredholm (T–F) deconvolution of SSITKA data for methanation over a Ru/SiO_2 catalyst. Two active pools of carbon—a highly active α and a less active β carbon form—were discerned from the reactivity distribution. The reactivity distribution also provides the average activities, $\bar{k}_\alpha$ and $\bar{k}_\beta$, and the peak areas, x_α and x_β, which indicate the relative sizes of each respective pool. The inverse-Laplace-transform method may result in shifting of the reactivity-distribution peak locations. However, it has been found to provide reasonable estimations of the relative pool sizes.[17] If the computational cost is tolerable, the T–F method may be used as an alternative in order to obtain more precise reactivity distributions.

IV. Mechanistic Assessments

SSITKA can provide insight into the possible catalyst-surface mechanism. Figure 11 presents the transient responses for an irreversible-reaction mechanism consisting of a single pool, two serial pools, or two parallel pools. It is seen in Figure 11 that, qualitatively, pools in series exhibit an S-shape transient response while the single- and parallel-pool models exhibit single-exponential and multiexponential behavior, respectively. An S shape for pools in series results because of the presence of the upstream pool through which the new isotopic label is distributed before it reaches the final pool in the pathway. In contrast, for a single pool the new isotopic label begins to immediately decay exponentially. For multiple pools in parallel, the resulting isotopic transient response does not exhibit S-shape behavior but an additive combination of exponentials. These catalyst-surface differences can be enhanced by looking at the transient behavior under partial isotopic exchange.[12] Partial isotopic exchange is accomplished by switching at time t_0 from the old label to the new label, R ⇒ *R, then back to the old label, *R ⇒ R, again at time $t_0 + \Delta t$. The result of these switches distinguishes the behavior of single-, serial-, or parallel-pool mechanisms as shown in Figure 12. As can be seen in this figure, following the switch back to the isotopic label, the transient responses of the single- and parallel-pool mechanisms immediately begin to increase following the switch. This

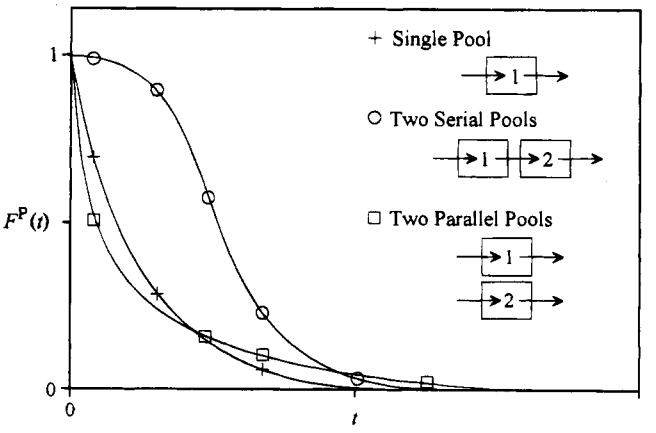

Figure 11. Typical transient responses for three catalyst-surface mechanisms. The responses have been corrected for gas-phase holdup.

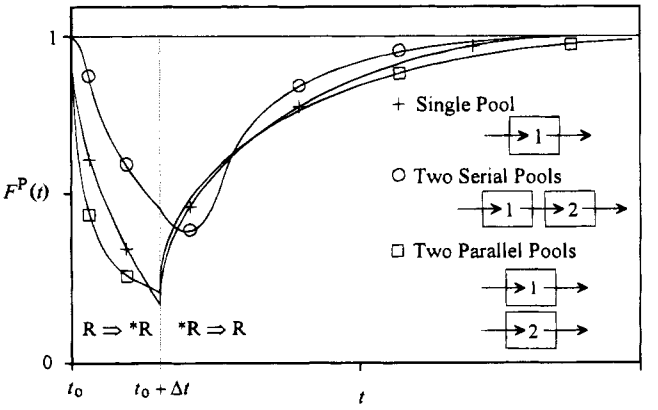

Figure 12. Partial isotopic-exchange transient responses.[12]

behavior is in contrast to the serial-pool mechanism where the transient response continues to decrease for a time following the switch before ultimately increasing. The reason for this behavior is due to the presence of the upstream pool which delays the reappearance of the old isotopic label following the switch back to the old isotope. This delay is not present in the single- and parallel-pool mechanisms. In addition, the method of partial isotopic exchange may be used to determine the individual residence times for two pools in parallel if one of the residence times of the pools is significantly greater than the other pool.[12] In this situation, if Δt is also significantly less than the greater residence time, then only the fast-filling pool (small residence time) will contain a substantial amount of the new isotopic label when the switch back to the old isotopic label occurs. Thus, the resulting transient response of the new isotopic label after the switch back to the old isotopic label will exhibit primarily the behavior of the fast pool allowing a separate analytical determination of its residence time. The residence time of the slow pool can then be determined from a fully exchanged isotopic experiment.

The parameter relationships for the possible mechanistic models given in Figure 7 were examined by Chen and Goodwin.[19] These models were used to analyze SSITKA results for ethane hydrogenolysis. Because reversible adsorption of the ethane reactant occurred, models 1 through 3 could be eliminated as possible mechanisms. Reversible adsorption of reactant could occur via models 4 and 5, as well as model 6 which represents the existence of two types of adsorptive sites—one reactive and the other nonreactive. It was determined by D_2-ethane exchange that model 6 could be excluded because no singly deuterated ethane was found in the effluent. However, the D_2-ethane exchange indicated that essentially all ethane adsorbed and either reacted to methane or desorbed back as ethane. Using $^{12}C/^{13}C$ isotopic labeling, the transient response of methane always exhibited a longer residence time than that of ethane; thus, model 4 was excluded since this model would result in equivalent transient responses for the ethane and the methane if all ethane was adsorbed. Consequently, model 5 was chosen as the most promising reaction mechanism.

If all of the isotopically labeled reactant can be assumed to have adsorbed on the catalyst surface for model 5, then the reactant transient response, $F^R(t)$, is equivalent to

$$F^R(t) = \exp(-t/\bar{\tau}_o^R) = \exp(-t/\bar{\tau}_1^A) \qquad (41)$$

where $\bar{\tau}_o^R$ is the mean residence time obtained from the reactant transient response. Thus, integration of the reactant transient response yields $\bar{\tau}_1^A$ since $\bar{\tau}_1^A = \bar{\tau}_o^R$, and $\bar{\tau}_2^A$ can be subsequently determined. If all of the reactant does not adsorb on the catalyst surface, then $\bar{\tau}_o^R$ determined from the reactant transient response, $F^R(t)$, represents only a minimum value and $\bar{\tau}_1^A \geq \bar{\tau}_o^R$.

V. Experimental Considerations

A. Reactor Choice—CSTR and PFR

Both continuous-stirred tank reactors (CSTR's) and plug-flow reactors (PFR's) have been used in SSITKA. The typical continuous-flow CSTR for heterogeneous catalysis studies utilizes a fixed catalyst bed with a well-mixed gas phase to obtain gradientless conditions. The various designs of mechanically assisted back-mixing and external-recycle reactors and their application in transient analysis can be found elsewhere.[7] The CSTR is typically operated at a high-recycle flow rate to maximize the superficial linear velocity through the catalyst bed to minimize any diffusional resistances external to the catalyst particles. However, these reactors often add experimental complexity and typically involve a considerable total reactor system volume relative to the catalyst-bed volume which increases the consumption of expensive isotopes and decreases their detectability. This makes it difficult to accurately ascertain the transient behavior of the catalyst surface.[7,20]

Due to the disadvantages in using a CSTR, it has become common in SSITKA to use plug-flow microreactors (micro-PFR's) because of their low reactor volume and operational simplicity. However, modeling of PFR's requires additional spatial-position variables which leads to increased complexity in their analysis.[21] Consequently, it has also become common to model the micro-PFR by assuming gradientless conditions in the catalyst bed, a condition which is analogous to a CSTR and obtainable in a micro-PFR.[20] The differential-bed micro-PFR utilizes a short residence time of reactant in the catalyst bed to obtain a differential conversion (<5%) of reactant and minimal reactant concentration gradients. This requirement unfortunately limits the operating ranges in reaction studies using micro-PFR's, and a CSTR remains the best reactor to avoid concentration gradients if it is desired to operate at higher conversions.

Alternative methods based upon the micro-PFR may be used to promote back-mixing within the catalyst bed to minimize concentration gradients. Increased back-mixing can be obtained by maximizing the bed's diameter-to-length ratio for a given volumetric feed rate.[22] However, this method results in lower superficial linear velocities which may introduce interparticle diffusional effects. Interparticle diffusional resistances are relatively easy to avoid by operating the reactor at a high superficial linear velocity through the catalyst bed. Thus, another method for minimization of concentration gradients is to introduce the reactant feed radially or within the catalyst bed via a back-flow mode to enhance back-mixing while maintaining a high superficial linear velocity through the bed.[15]

A final consideration, and possibly the most important, in choosing either a CSTR or a PFR is whether adsorption effects are exhibited by reactants and/or products, and this will be addressed in a subsequent section.

B. Gas-Phase Holdup Correction

When evaluating the transient response of an isotopically labeled species measured at the reactor outlet, two latent contributing sources—the reactor and the catalyst surface—must be considered in the transient response modeling and analysis. There are two methods which have been used in the application of an inert tracer for gas-phase holdup determination in SSITKA.

The *first method* is composed of two separate determinations. The "nonideality of the step input" is determined based on the inert-tracer transient response of an empty reactor assumed to be operated under identical conditions as the reactor containing the catalyst. This forcing function is then used in subsequent analysis. Likewise, the "back-mixing" attributable to the catalyst bed is determined using a separate inert-tracer step input to the catalyst bed, and the resulting transient response is termed the mixing function. Empirical curve fitting of the forcing function and the mixing function, typically using multiple-CSTR models, permits determination of their individual transient behavior, and this method has been used to verify CSTR behavior in a micro-PFR using a large diameter-to-length catalyst bed designed to promote back-mixing as a CSTR.[23]

The *second method* for gas-phase holdup determination is the inclusion of a small concentration of the inert tracer in one of the inlet streams during the isotopic switch (Figure 2).[11] This inert-tracer transient response contains both transient contributions of the nonideal step input and the back-mixing within the reactor and the catalyst bed.

A nonadsorbable inert tracer (such as Ar or He), distinguishable from any inert diluent in the feed streams, is typically used for determination of the gas-phase holdup. System linearity is maintained if a only small amount of inert tracer is used, and with the sensitivity of a mass spectrometer this requirement is easily met. It is also assumed that the mass, momentum, and heat transport properties of the inert tracer are identical to the reactant and product species. The difference between the measured inert-tracer and isotopic-tracer transient responses is attributable to residence time on the catalyst surface. It can be shown by mass balance that the mean surface-residence time, $\bar{\tau}^{P}$, is obtained from

$$\bar{\tau}^{P} = \bar{\tau}^{P}_{m} - \bar{\tau}^{I}_{g} \tag{42}$$

where the $\bar{\tau}^{P}_{m}$ and $\bar{\tau}^{I}_{g}$ are obtained by integration of the respective isotopic- and inert-tracer transient responses and are equivalent to the areas under each response as indicated in Figure 13, parts a and b. Subscript m indicates the measured or observed response, and subscript g refers to the gas-phase holdup. Consequently, the mean surface-residence time, $\bar{\tau}^{P}$, can *always* be determined from the measured isotopic- and inert-tracer transient responses. In Figure 13, parts a and b, the rectangular area under the inert-tracer transient response to the left of time t_o is the gas-phase holdup attributable to pure time delay of the gases in the system while the area to the right of time t_o is attributable to the system nonidealities including back-mixing and the nonideal

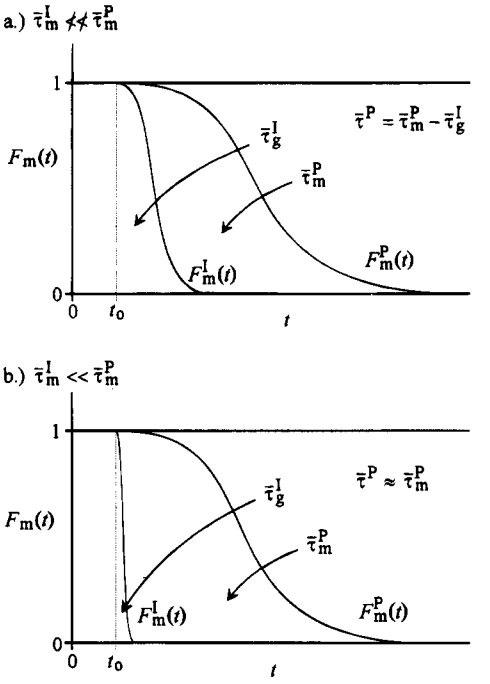

Figure 13. Relative importance of gas-phase holdup correction based upon the magnitudes of the inert-tracer and isotopic-tracer mean residence times.

step input. Usually, the time-delay part of the gas-phase holdup is ignored by only considering events after $t = t_o$.

It is useful to note the relative importance of gas-phase holdup correction since $\bar{\tau}^{I}_{g}$ depends upon the type of reactor used, the flow characteristics of the system, and the magnitude of $\bar{\tau}^{P}$ (thus $\bar{\tau}^{P}_{m}$) for the reaction. In Figure 13a, it is evident that the magnitude of the inert-tracer mean residence time, $\bar{\tau}^{I}_{g}$, approaches that of the isotopic-tracer mean residence time, $\bar{\tau}^{P}_{m}$. Consequently, the measured isotopic transient *must* be corrected for gas-phase holdup in order to obtain the true overall mean residence time for the surface intermediates. However, for the relative transient responses indicated in Figure 13b, $\bar{\tau}^{I}_{g} \ll \bar{\tau}^{P}_{m}$, the contribution by the gas-phase holdup has a minimal effect on the measured isotopic-transient response, and $\bar{\tau}^{P} \approx \bar{\tau}^{P}_{m}$.

Reactivity distribution analysis and mechanistic determinations require that the catalyst-surface transient response, $F^{P}(t)$, be obtained by gas-phase holdup correction of the measured transient response. Removal of the gas-phase holdup requires proper modeling in order to obtain a minimal loss of information without the introduction of extraneous model effects which could result in a specious catalyst-surface response. The general equation for gas-phase holdup correction and, thus, for determination of the transient response attributable to the catalyst surface, $F^{P}(t)$, from a measured isotopic-transient response, $F^{P}_{m}(t)$, is[24]

$$F^{P}(t) = F^{P}_{m}(t) + c^{I}_{g_1}\frac{dF^{P}_{m}(t)}{dt} + c^{I}_{g_2}\frac{d^2F^{P}_{m}(t)}{dt^2} + \ldots + c^{I}_{g_n}\frac{d^nF^{P}_{m}(t)}{dt^n} \tag{43}$$

where $c^{I}_{g_i}$'s are n constant coefficients determined from the measured inert-tracer transient response, $F^{I}_{m}(t)$. If the overall reactor can be characterized as an n number of equal CSTR's in series, then

$$c^{I}_{g_i} = \frac{1}{i!}(\bar{\tau}^{I}_{g})^{n}\prod_{j=0}^{i-1}(n-j) \qquad i = 1, 2, 3, ..., n \qquad (44)$$

where $\bar{\tau}^{I}_{g}$ is the mean residence time for each individual CSTR. If $n = 1$, then eq 43 reduces to

$$F^{P}(t) = F^{P}_{m}(t) + \bar{\tau}^{I}_{g}\frac{dF^{P}_{m}(t)}{dt} \qquad (45)$$

which is applicable *only* for gas-phase holdup correction of a single ideal CSTR.[15] In applying eq 43 to plug-flow reactor (PFR) systems, the number of required terms becomes large, approaching infinity for an ideal PFR. Unfortunately, the use of even several terms still leads to substantial error because of the inherent inaccuracies in higher-order numerical differentiation. However, eq 45 *should not* be used for PFR systems, including differential micro-PFR's, since it also neglects the higher-order terms of eq 43 and can lead to substantial error in the gas-phase holdup correction. Therefore, while eq 42 can still be used regardless of the reactor type, more robust methods need to be developed for gas-phase holdup correction of transient responses obtained from PFR's if analytical methods requiring the corrected transient response, such as reactivity-distribution analysis and transient-response curve fitting, are to be applied more correctly in SSITKA. However, if $\bar{\tau}^{I}_{g}$ is relatively small ($\bar{\tau}^{I}_{g} \ll \bar{\tau}^{P}_{m}$, Figure 13b) then the effects of gas-phase holdup and back-mixing can be ignored in analyses without introducing excessive error. Consequently, model parameters can be obtained using common numerical techniques such as iterative curve fitting of the measured transient responses.[21]

C. Isotopic Effect

The mechanistic modeling and kinetic parameter determinations in SSITKA assume that steady-state reaction conditions are maintained by the method of isotopic substitution. This is not the situation for hydrogen/deuterium (H/D) isotopic exchanges, such as H_2/HD, CH_4/CH_3D, or C_2H_6/C_2H_5D, because of the kinetic and thermodynamic differences arising from the relatively large mass differences and bonding energies between hydrogen isotopes.[25] Therefore, caution must be exercised when interpreting H/D isotopic-based transient responses because the kinetic rates and surface intermediates may be substantially displaced from steady state following the isotopic switch. However, H/D exchanges remain useful for indicating or identifying bond breakages within a particular molecular species following adsorption−desorption or reaction. The isotopic effect lessens as the mass of the isotope increases, and the isotopic effects for reactions involving $^{12}C/^{13}C$, $^{14}N/^{15}N$, or $^{16}O/^{18}O$ are minimal.

D. Diffusion Effects

Concentration gradients in the catalyst bed (interparticle) or within the catalyst particles (intraparticle) may result from diffusional effects and substantially affect the transient responses which interferes with the determination of the underlying kinetic parameters attributable to the catalyst-surface reaction. The presence of interparticle or external diffusional effects can often be determined experimentally by varying the gas space velocity. These effects can be relatively easily avoided by operating at high space velocities through the catalyst bed. However, intraparticle or pore diffusion may not be readily avoidable and is dependent upon the diffusivities of the gases, the reaction rate and stoichiometry, and the catalyst physical parameters including pore size, porosity, tortuosity, and particle diameter. The presence of intraparticle diffusional effects can be determined experimentally by varying the catalyst-particle diameter.

It is usually desirable to avoid intraparticle diffusional effects in order to obtain the true intrinsic reaction rate, and this may be accomplished by using very small diameter catalyst particles (low Thiele modulus) or, if possible a nonporous support. For SSITKA mean residence-time resolutions down to 1 s, catalyst-particle diameters of $\ll 10^{-2}$ cm should be used to limit diffusional effects based upon a typical effective diffusivity of $D_e = 10^{-3}$ cm^2/s for porous silica or alumina supported catalysts.[3]

Because of the short transient response times, it is difficult to use SSITKA to measure the diffusivities associated with catalyst supports such as porous and nonporous silica or alumina. However, given the low intracrystalline diffusivities of molecules in zeolites, it may be possible to use isotopic transients to investigate diffusional effects in zeolites.[26]

Since little work has been done in the application of SSITKA to studying diffusional effects, this remains an important area for future development and application of SSITKA where the determination of both diffusional and kinetic parameters at steady-state reaction conditions might be able to be accomplished.

E. Adsorption Effects

1. Reactant Adsorption—Chromatographic Effect

A chromatographic effect has been observed in PFR's for the transient responses of strongly adsorbing, fast-equilibrating reactant species such as CO in CO hydrogenation.[11] Figure 14 indicates this effect where the isotopic transient response of the CO reactant does not simultaneously appear with the Ar inert-tracer transient response but appears later, paralleling the Ar response. This holdup was at-

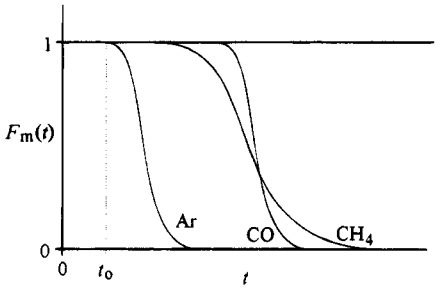

Figure 14. Chromatographic effect in CO hydrogenation.[11]

tributed to equilibrated adsorption−desorption of the ^{13}CO with a large reservoir of ^{12}CO adsorbed on the catalyst which required a finite time to be displaced by the ^{13}CO. A similar effect was observed for H_2/D_2 exchanges in NH_3 synthesis studies[15,27] which was due to adsorption/absorption on/in the reactor walls that resulted in a large reservoir of H_2 in the reactor system. Likewise, benzene exchanges in benzene hydrogenation[28] exhibited a chromatographic effect where both benzene and cyclohexane adsorbed readily on the reactor walls and within the catalyst bed. The presence of these large reservoirs for adsorption/desorption results in isotopic concentration gradients within the reactor system or along the catalyst-bed length which is exhibited as a chromatographic effect following the isotopic switch. This complicates the interpretation of the product-species transient responses, and simplified corrections have been applied in the analysis of transient responses involving a chromatographic effect.[28] The isotopic concentration gradients may be minimized in a PFR by operating at high space velocities; however, if a large adsorption reservoir is present, the chromatographic effect cannot be avoided.[29] Consequently, a CSTR reactor is then preferred to eliminate any isotopic concentration gradients with respect to the catalyst bed and simplify the interpretation of the transient responses.[15]

2. Product Readsorption

The effects of readsorption in SSITKA are perhaps the most difficult to avoid or interpret, and the presence of readsorption can lead to substantial contributions to the transient responses and interfere with the determination of the underlying kinetics of the catalyst surface. If readsorption of product occurs or another species adsorbs at the reactive sites, then there is a reduced activity and reaction rate. If readsorption of product occurs at nonreactive sites, the activity will not be affected; however, the abundance of surface intermediates leading to product determined from the transient rate response will be the sum from both the reactive and nonreactive adsorption sites. Hence, the mean surface-residence time attributed to the reaction will be overestimated, and the reactivity will be underestimated. Even if product does not readily adsorb, multiple adsorptions of reactant prior to reaction can lead to overestimations of the mean surface-residence time.

Decreasing the bed length, L_b, or increasing the weight hourly space velocity, WHSV, tends to minimize interparticle readsorption in the catalyst bed. However, if too low an L_b/D_b ratio (D_b is the bed diameter) is used, substantial channeling in the catalyst bed may occur resulting in erroneous interpretations. An increase in the specific reaction rate with decreasing bed length indicates the presence of readsorption at the reactive sites. Therefore, one often performs a series of experiments at various flow rates (WHSV's) or catalyst loadings (bed lengths, L_b's) and extrapolates to negligible readsorption (see Figure 15) to obtain the intrinsic reaction rate or true mean surface-residence time, $\bar{\tau}^P_{sur}$, which is equivalent to $\bar{\tau}^P$ for reaction. If readsorption occurs only at nonreactive sites, decreasing the bed length does not affect the specific reaction rate but results in a

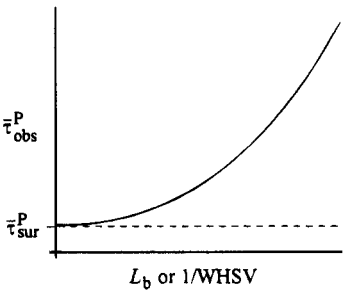

Figure 15. Experimental determination of the mean surface-residence time in the presence of adsorption.

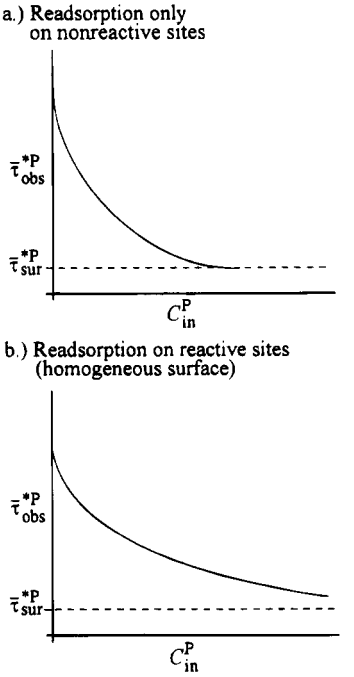

Figure 16. Mean-residence-time readsorption behavior upon addition of unlabeled product in the inlet stream.

decrease in the observed mean residence time, $\bar{\tau}^P_{obs}$, which upon extrapolation still yields $\bar{\tau}^P_{sur}$. Unfortunately, these methods do not reveal the presence of, nor decrease, intraparticle readsorption within the pore system of the catalyst particles.

An experimental method which may elucidate the presence of both interparticle or intraparticle readsorption is the addition of unlabeled product to the feed stream to compete for readsorption sites with the labeled product formed by reaction. If readsorption of product occurs only at nonreactive sites, increasing the amount of unlabeled product, C^P_{in}, at the reactor inlet will decrease the observed mean residence time, $\bar{\tau}^{*P}_{obs}$, determined from the labeled transient response, ultimately reaching a limiting value, $\bar{\tau}^{*P}_{sur}$, (Figure 16a) which is equivalent to the mean surface-residence time, $\bar{\tau}^P$, for reaction. If readsorption occurs only on the reactive sites, then the observed mean residence time, $\bar{\tau}^{*P}_{obs}$, will only asymptotically approach a limit (Figure 16b) as the reaction rate decreases, especially if the catalyst is porous. However, it should be noted that, if the surface active sites exhibit adsorption heterogeneity, this behavior may become more complex requiring further interpretation.

Micro-PFR's typically have the advantages over CSTR's of a shorter residence time of the gas-phase species in the catalyst bed and lower gas-phase concentrations which tend to decrease interparticle readsorption. However, even at differential conversion of reactant (<5%) in a micro-PFR, substantial product concentration gradients may develop. If readsorption for a reactant or product species is inherently intrusive in the determination of the true catalyst-surface reaction behavior, such as in ammonia synthesis where NH_3 is in equilibrium with the catalyst surface, then a CSTR may be preferred due to the absence of concentration gradients.[15]

VI. Reactions Studied

To date, SSITKA has contributed significantly to our understanding of a wide range of surface-catalyzed reactions (see Table 1) including CO hydrogenation, ammonia synthesis, ammonia oxidation, CO oxidation, NO–CO reaction, methane activation, propylene partial oxidation, ethane hydrogenolysis, benzene hydrogenation, isobutene hydrogenation, isobutane dehydrogenation, propane dehydrogenation, and vinyl acetate synthesis. While meant to be illustrative and not definitive, we believe that this table includes most of the important SSITKA studies employing this technique to date. Issues explored

Table 1. Reactions Studied by Steady-State Isotopic-Transient Methods

reaction	catalyst	ref(s)
methanation and Fischer–Tropsch synthesis	Fe	30, 31[a]
	Fe/Al_2O_3	32
	Co	3, 11, 29, 33[b]
	Co/Al_2O_3	34,[c] 35,[d] 36[d]
	Co/SiO_2	31, 37, 38, 39[e]
	Ni	12,[f] 40,[f] 41,[f] 42
	Ni/Al_2O_3	22, 23
	Ni/SiO_2	3, 11, 40,[g] 43,[g] 44,[g] 45,[g] 46,[g] 47
	Ru/Al_2O_3	3, 11, 29, 37, 48, 49
	Ru/SiO_2	16, 17, 50, 51, 52, 53,[h] 97
	Ru/TiO_2	16, 54, 55
	Rh/MgO	56
	Rh/Al_2O_3	57, 58, 59
	Rh/SiO_2	33,[b] 60,[b] 61,[i] 62[b]
	Pt/TiO_2	47
ammonia synthesis	Fe	15,[j] 27[j]
	Ru/SiO_2	63[j]
ammonia oxidation and NO selective catalytic reduction	V_2O_5	64, 65
ethane hydrogenolysis	Co/SiO_2	66
	Ru/SiO_2	19
methanol synthesis	Pd/SiO_2	67, 68[k]
benzene hydrogenation	Ni	28, 70[l]
	Ni/SiO_2	28, 70[l]
methane coupling	MgO	71,[k] 72, 73
	Li/MgO	72, 73, 74, 75
	TiO_2	76[k]
	NiO	73
	Sr/La_2O_3	77
	SnO_2	73
	Sn/MgO	73
	La_2O_3	69, 71,[k] 77
	Sm_2O_3	73, 75, 78, 79
methane partial oxidation	V_2O_5/Al_2O_3	80[m]
	V_2O_5/SiO_2	80,[m] 81, 82
	MoO_3	83[n]
	MoO_3/SiO_2	84[n]
	Pr_6O_{11}	85[b]
	Sm_2O_3	85,[b] 86,[b] 87,[b] 88[b]
	Li/Sm_2O_3	85[b]
NO–CO reaction	Rh/La_2O_3	89
	$Pt/Rh/NiO/CeO_2/Al_2O_3$	89[o]
CO oxidation	Rh/La_2O_3	89
	$Pt/Rh/NiO/CeO_2/Al_2O_3$	89[o]
propylene partial oxidation	Sb/Sn/V Oxide	90
propane dehydrogenation	Pt/Al_2O_3	91
	$Pt/Sn/Al_2O_3$	91
isobutene hydrogenation and isobutane dehydrogenation	Cr_2O_3	92,[p] 93[p]
vinyl acetate synthesis	$Pd/Cd/K/SiO_2$	94
	$Pd/Au/K/SiO_2$	94
ethylene hydroformylation	Rh/SiO_2	95,[b] 96[b]

[a] Promoted (SiO_2/Cu/K) Fe. [b] Pulse technique. [c] Pt or Re promoted. [d] La promoted. [e] Zr promoted. [f] Raney nickel. [g] Commercial–kieselguhr support. [h] K doped. [i] V promoted. [j] Commercial–promoted (Al_2O_3/K_2O/CaO) Fe catalyst. [k] Li promoted. [l] Also Ni and $Ni–K/SiO_2$. [m] Also bulk and supports. [n] Various molybdena species. [o] Commercial–automotive catalyst. [p] Chromia gel.

using SSITKA have included such things as the role of lattice oxygen in partial oxidation, mechanisms or pathways of reaction, the presence and implications of site heterogeneity, the role of chemical promoters, the effect of temperature and partial pressure of reactants on surface coverage of intermediates, and the consequence of readsorption of products on reaction. Due to space limitations, only the most significant findings of the representative reactions of ammonia synthesis, CO hydrogenation, ethane hydrogenolysis, and methane activation are given. These reactions, however, include those which have been studied the most by SSITKA (CO hydrogenation and methane activation). Citations have been chosen primarily to show how SSITKA has been used to discern information about catalyst systems. The reader is referred to the original papers cited in Table 1 for complete details of the findings for all of the reactions studied.

A. Ammonia Synthesis

SSITKA has been used to study ammonia synthesis at temperature and pressure on a commercial ammonia synthesis Fe catalyst (Haldor Topsoe KMIR).[27] The results suggested that *N is the most abundant reactive intermediate on the surface during steady-state reaction. Analysis of the ammonia isotopic transients by inspection (using a semilog plot)[15] and by the inverse Laplace transform method[16] indicated that the reactive surface exhibited site heterogeneity, especially above 700 °C. This is not surprising considering that KMIR contains a number of promoters.

In a more recent paper, Nwalor and Goodwin[63] reported the results of a study of K promotion of Ru. It is well known that K promotion greatly increases the rate of ammonia synthesis on Ru catalysts, and it had been previously suggested by numerous investigators that this increase in the rate was due to a promotion of N_2 dissociation or to an increase in surface intermediates. By using SSITKA, Nwalor and Goodwin were able to show that the increase in rate was due primarily to the creation of a set of "super" active sites rather than an increase in the number of reactive surface intermediates. While all the sites on the catalyst showed some increase in activity upon promotion, the "super" active sites exhibited activities more than an order of magnitude higher. While constituting only 20% of the active sites/intermediates, these "super" active sites accounted for 78% of the reaction in the promoted catalyst.

B. CO Hydrogenation

1. Hydrocarbon Synthesis

One of the earliest SSITKA studies of CO hydrogenation was that of Happel *et al.*[43] By using transient isotopic tracing of ^{13}CO, ^{18}O, and D, they were able to establish that carbon dioxide formation during methanation on a Ni catalyst appeared to occur directly and not via the water-gas-shift reaction.

Biloen *et al.*[11] found by studying a series of Ni, Co, and Ru catalysts that only a small fraction of the carbidic overlayer on the catalyst surfaces belonged to the active intermediates. Their results suggested that both methane and higher hydrocarbons were formed from a common pool of intermediates, probably C_1.

Numerous studies have addressed this issue of surface coverage during CO hydrogenation. In general, regardless of whether the catalyst employed is Co, Rh, Ni, Fe, Ru, or Pt, the active catalyst surface is primarily covered by reversibly adsorbing CO and low-activity carbidic species. Only a small fraction (typically <10%) is covered by active surface intermediates of methane or higher hydrocarbons.[11,32,33,39,51,53,55,57-59] However, Mims[38] has found that the active surface carbon on a Co/silica catalyst is common to both methanol and hydrocarbon products. He suggests that this intermediate possesses the original C−O bond but is different from adsorbed CO.

Using SSITKA, Stockwell *et al.*[32] were able to show that for Fischer−Tropsch synthesis on an Fe/Al_2O_3 catalyst, bulk carbide did not participate significantly in the formation of products.

In perhaps the first SSITKA study to address the role of promoters in a catalyst, Yang *et al.*[40] were able to conclude that the structural promoter Al_2O_3 in Raney Ni increases the activity of the catalyst by increasing the surface abundance of intermediates rather than by changing their reactivity. Soong and Biloen[41] also investigated the aging of a Raney Ni catalyst during methanation. They were able to suggest, on the basis of isotopic transients taken at various times-on-stream, that loss of activity was due to a decrease in the most active intermediates. Their results clearly indicated the existence of two pools of intermediates, one 7 times more reactive than the other.

Chain growth during Fischer−Tropsch (F−T) synthesis has been the subject of a number of studies.[29,31,48,49,54,55] Mims and co-workers[31,48,49] have found that the reactive carbon appears to spend most of its lifetime on the catalyst surface as C_1 species. However, after formation of C_2 species, chain growth is rapid.[48] In addition, chain growth was found to be best described by terminal addition to what becomes the olefinic end of the hydrocarbon molecule. Krishna and Bell[54] were able to show clearly that ethylene can initiate chain growth as well as serve as a source of C_1 monomer species for additional chain propagation.

Goodwin and co-workers[35,36,39,53,97] have addressed the influence of promoters on hydrocarbon synthesis. Hoost and Goodwin[53] found that K promotion of Ru resulted in a decrease in overall activity due to the decrease in reactivity of both the C_1 (high activity) and C_1 (low activity) intermediates. Deactivation with time-on-stream was due solely to the decrease in surface concentration of the active intermediates and not to a change in the reactivity of the intermediates. On the basis of a separate study using both CO hydrogenation and ethane hydrogenolysis, Hoost and Goodwin[97] suggested that K promotion affects

the carbidic overlayer by regulating the catalyst's hydrogenation capabilities.

La has been suggested to be useful as a chain growth promoter for Co F−T catalysts. La promotion of Co/Al_2O_3 was found to decrease the selectivity of methane.[35,36] Low levels of La promotion increased the activity of the catalyst. However, for La/Co > 0.1, there was a decrease in overall catalyst activity. The affect on activity seemed to be related especially to a change in surface concentration of the active intermediates. Deconvolution of the isotopic transients indicated that La promotion affects methane site activity by increasing the reactivity of the most active pool of intermediates.

Zr, on the other hand, has been shown to be a significant rate promoter for Co/SiO_2 as well as a selectivity promoter at high loadings.[39] The effect on rate is especially great initially. This initial rate increase is a function of both an increase in reactivity and an increase in surface concentration of the intermediates. However, both of these parameters decline significantly with time-on-stream.

2. Oxygenate Synthesis

Methanol synthesis on Li-promoted Pd/SiO_2 has been studied by SSITKA.[67,68] Li is well known to be a methanol rate promoter for Pd. The SSITKA results indicated that the surface concentration of active intermediates increased upon promotion, although the site/intermediate activity decreased. However, because the increase in surface concentration was so much greater than the decrease in activity, the rate of methanol formation increased.

Koerts and van Santen[61] investigated the effect of vanadium promotion of Rh/SiO_2. They found that ethanal formation appeared to occur at two different types of sites. V promotion decreased the desorption rate of ethanal while enhancing its hydrogenation to ethanol. Although V did not affect the rate of CO insertion into surface CH_x species, it did increase the concentration of active oxygenated species.

By using a variation of SSITKA, Chuang *et al.*[62] has been able to show why an increase in reaction pressure results in the increased formation of oxygenated species such as acetaldehyde on Rh catalysts. With increasing pressure, the surface-residence time of CH_x species increases permitting the greater insertion of CO.

C. Ethane Hydrogenolysis

Ethane hydrogenolysis has been studied by SSITKA on both Ru[19] and Co.[66] Chen and Goodwin[19] have developed mathematics and methodology for handling a reaction such as this which includes reversible steps. They were able to show that ethane hydrogenolysis can be modeled as two intermediate pools in series—the first consisting of dicarbon species and the second monocarbon species. The surface concentration and reactivity of intermediates for each of these pools were able to be estimated. The surface coverage of monocarbon species increased with temperature while that of dicarbon species remained constant. The activation energies of the surface reactions of di- and monocarbon species were estimated to be ca. 36 and 9 kcal/mol, respectively. The former is similar to the overall activation energy for ethane hydrogenolysis on Ru, suggesting that C−C bond breakage is the rate-limited step. The activation energy for the reaction of monocarbon species is typical of hydrogenation reactions.

Ethane hydrogenolysis was used to help characterize the effect of aqueous impregnation on Co/SiO_2. Aqueous impregnation and drying of a reduced and passivated Co/SiO_2 catalyst led to the formation of Co silicate. SSITKA indicated that the surface concentration of active intermediates during ethane hydrogenolysis declined as a result of the changes in the catalyst. The pseudo-first-order rate constants, on the other hand, increased slightly, probably due to the reduction in the size of the Co−metal particles.

D. Methane Activation

1. Coupling

Methane activation, of all the reactions studied, has perhaps been the biggest challenge for SSITKA due to the high temperatures required. At temperatures in excess of 550 °C, surface residence times of reactive intermediates would be expected to be very low, perhaps below the detectability limit of the technique. Ekstrom and Lapszewicz[85−88] were the first to successfully demonstrate that information could be gathered by SSITKA for this reaction. For a number of rare-earth catalysts, they were able to conclude that the reaction involves only a small number of active sites, that gas-phase oxygen rapidly exchanges with lattice oxygen, and that methane conversion is dependent on the rate of lattice-oxygen exchange. Because of the methodology used by them, accurate surface-residence times for carbon leading to ethane were not able to be determined. However, Peil *et al.*[72,74,75,78,79] were able to determine surface-residence times for the carbon in the products for Li/MgO and Sm_2O_3. On Sm_2O_3, the surface-residence time for carbon leading to ethane was 4 s at a reaction temperature of 600 °C. However, the residence times for CO and CO_2 were only 2−3 s, suggesting that the nonselective products can be made directly and are not just secondary products of methyl radicals or ethane. Methane was shown to adsorb reversibly for a detectable time for temperatures <650 °C on all active catalysts.[72,75,78]

The oxygen reaction pathway has also been explored by SSITKA. Lattice oxygen was shown to be important in determining the rate of methane activation.[74] Peil *et al.*[73] provide a discussion of how lattice-oxygen diffusivities can be determined under reaction conditions.

2. Partial Oxidation

The partial oxidation of methane offers interesting possibilities since the valuable chemicals, methanol and formaldehyde, are formed directly. A number of studies have been reported which utilized SSITKA to study this reaction on supported and unsupported vanadia,[80,81,82] molybdena,[83] and silica-supported molybdena.[84] Methane was found to adsorb reversibly only if a catalyst was active for reaction.[81] It was speculated that different types of "sites" involved in

the formation of HCHO, CO, and C_2H_6 may correspond to vanadium oxide species in different redox states. While secondary reaction of HCHO has been shown to result in CO, the SSITKA results indicated that readsorption of HCHO was irreversible, leading to the nonselective product. Results indicate significant exchange of oxygen between the support and the active phase for silica-supported vanadia[80] and molybdena.[84] The redox nature of vanadia/silica was evidenced by the increase in lattice oxygen exchange in the presence of methane.[80]

VII. Future Directions for SSITKA

Research is proceeding on numerous aspects of SSITKA. Theoretical work in our laboratories is aimed at improving gas-phase holdup subtraction and developing a mathematical model for the isotopic transients observed.[24] Improvement of gas-phase holdup subtraction will enable the technique to be better applied to the study of heterogeneously catalyzed reactions having surface intermediates with short residence times. The development of a mathematical model will provide us with the ability to evaluate the impact of various processes on the isotopic transients.

An investigation in our laboratories has just begun to better understand the effects of readsorption/diffusion of reactants and products on the transients. It is possible that more information about these processes will be able to be derived directly from the transients in the future.

Russell *et al.*[98] have shown by calculations that SSITKA should be able to be applied to reaction on a catalyst surface from the liquid phase provided certain requirements are met. This obviously presents significant challenges due the inherent greater residence time in a reactor for liquid-phase reactions. However, for certain liquid-phase reactions, application of SSITKA would seem to be possible, even if perhaps more limited than for gas-phase reactions.

Finally, the list of gas-phase reactions studied by SSITKA has been growing steadily since the middle 1980s when only CO hydrogenation had been addressed. This list will undoubtedly grow and be applied to more complex reactions, such as reported in the recent paper on the synthesis of vinyl acetate.[94] In theory, the primary limitations are the cost of isotopes, the complexity of the product mixture and its analysis by mass spectrometry, and the surface residence times of the intermediates. However, by the use of discrete effluent sampling on line followed by gas chromatography, reaction to convert products to species more amenable to isotopic analysis, and mass spectrometry, the second limitation has been able to be effectively overcome for the Fischer–Tropsch synthesis.[32,55] Another approach has been to use GC-MS combined with NMR for product analysis to determine ^{13}C location in a hydrocarbon molecule.[31]

VIII. Summary

SSITKA is a powerful technique for the kinetic study of heterogeneous catalytic reactions and has been used in a number of studies to determine *in situ* kinetic information about the catalyst-surface reaction intermediates and mechanisms at steady state. Other transient methods such as stop-flow techniques, often result in substantial disturbance of the catalyst-surface behavior, something which does not occur in SSITKA.

Table 2 summarizes the steady-state kinetic parameters which have been determined from SSITKA. The certainty in the parameter determination decreases in descending order in the table. The most general steady-state kinetic parameters which are determined from SSITKA are the abundances, $\bar{N}^P$, and overall mean residence time, $\bar{\tau}^P$, of the catalyst-surface reaction intermediates which lead to a particular product. SSITKA permits determination of these parameters independent of the underlying kinetic mechanism of the reaction. Through mechanistic assumptions and modeling, other steady-state kinetic parameters which can be determined from SSITKA include surface concentrations of different types of adsorbed reaction intermediates, coverages, surface lifetimes, turnover frequencies, site heterogeneity, activity distributions, and identification of possible mechanisms. SSITKA also provides the ability to determine the effects of different preparation methods, supports, promoters, and poisons on the steady-state behavior of catalysts. While providing fundamental catalytic information, SSITKA is also suitable for the characterization of commercial catalysts at industrial reaction conditions.[27]

Since SSITKA is a relatively new technique (in use less than 15 years) and has been shown to be a powerful method for determining steady-state kinetic mechanisms and parameters, it is expected be applied with increasing frequency, especially as it is introduced into new areas of reaction study. SSITKA

Table 2. Most Common Steady-State Kinetic Parameters Determined by SSITKA

kinetic parameters	assumptions	comments
abundance of adsorbed surface intermediates leading to P: $\bar{N}^P$ mean surface-residence time of adsorbed intermediates leading to P: $\bar{\tau}^P$	a single reactant isotopic element is incorporated per single product species	determined value is independent of the underlying kinetic model; however, any detailed value is dependent upon an assumed kinetic model
reactivity: k	overall reaction is pseudo-first order	parameter underestimation occurs for reversible-reaction pathway
surface coverage of adsorbed intermediates leading to P: $\bar{\theta}_c^P$	accurate number of active sites is obtainable from separate measurement	measured number of sites may be different than the true number of active sites, i.e., if obtained from chemisorption
reactivity distribution: $f(k)$	surface consists of pseudo-first-order parallel pools (a heterogeneous surface)	proper gas-phase holdup correction of the measured product-species transient response is required

has the potential for determining additional kinetic parameters which are difficult to measure, or cannot currently be measured, including those for reactions in zeolites and others principally affected by mass-transfer resistances. In addition, liquid-phase reactions may theoretically be studied[3] including those catalyzed by immobilized enzymes.[98]

Acknowledgments. This work was funded under National Science Foundation Grant no. CTS-9312519.

IX. References

(1) Happel, J. *Chem. Eng. Sci.* **1978**, *33*, 1567.
(2) Bennett, C. O. In *Catalysis Under Transient Conditions*, Bell, A. T., Hegedus, L. L., Eds.; ACS Symposium Series; American Chemical Society: Washington, DC, 1982; Vol. 178, p 1.
(3) Biloen, P. *J. Mol. Catal.* **1983**, *21*, 17.
(4) Kobayashi, H.; Kobayashi, M. *Catal. Rev.-Sci. Eng.* **1974**, *10* (*2*), 139.
(5) Bennett, C. O. *Catal. Rev.-Sci. Eng.* **1976**, *13* (*2*), 121.
(6) Schwarz, J. A.; Falconer, J. L. *Catal. Today* **1990**, *7* (*1*), 1.
(7) Happel, J. *Isotopic Assessment of Heterogeneous Catalysts*; Academic Press: Orlando, FL, 1986.
(8) Le Cardinal, G.; Walter, E.; Bertrand, P.; Zoulalian, A.; Gelus, M. *Chem. Eng. Sci.* **1977**, *32*, 733.
(9) Smith, J. M. *Chemical Engineering Kinetics*, 3rd ed.; McGraw-Hill: New York, 1981.
(10) Boudart, M. *AIChE J.* **1972**, *18*, 465.
(11) Biloen, P.; Helle, J. N.; van den Berg, F. G. A.; Sachtler, W. M. H. *J. Catal.* **1983**, *81*, 450.
(12) Soong, Y.; Krishna, K.; Biloen, P. *J. Catal.* **1986**, *97*, 330.
(13) Park, S. W.; Himmelblau, D. M. *Chem. Eng. J.* **1982**, *25*, 163.
(14) Happel, J.; Walter, E.; Lecourtier, Y. *Ind. Eng. Chem. Fund.* **1986**, *25*, 704.
(15) Nwalor, J. U. Ph.D. Dissertation, University of Pittsburgh, Pittsburgh, PA, 1988.
(16) de Pontes, M.; Yokomizo, G. H.; Bell, A. T. *J. Catal.* **1987**, *104*, 147.
(17) Hoost, T. E.; Gocdwin, J. G., Jr. *J. Catal.* **1992**, *134*, 678.
(18) Scott, K. F.; Phillips, C. S. G. *J. Chromatogr. Sci.* **1983**, *21*, 125.
(19) Chen, B.; Goodwin, J. G., Jr. Isotopic Transient Kinetic Analysis of Ethane Hydrogenolysis on Ru/SiO_2. *J. Catal.*, in press.
(20) Huang, Y.-J.; Lee, P.-I.; Schwarz, J. A.; Heydweiller, J. C. *Chem. Eng. Commun.* **1985**, *39*, 355.
(21) Happel, J.; Walter, E.; Lecourtier, Y. *J. Catal.* **1990**, *123*, 12.
(22) Stockwell, D. M.; Bennett, C. O. *J. Catal.* **1988**, *110*, 354.
(23) Stockwell, D. M.; Chung, J. S.; Bennett, C. O. *J. Catal.* **1988**, *112*, 135.
(24) Shannon, S. L. Ph.D. Dissertation, University of Pittsburgh, 1995.
(25) Ozaki, A. Isotopic Studies of Heterogeneous Catalysis; Academic Press: New York, 1977.
(26) Efstathiou, A. M.; Suib, S. L.; Bennett, C. O. *J. Catal.* **1992**, *135*, 223.
(27) Nwalor, J. U.; Goodwin, J. G., Jr.; Biloen, P. *J. Catal.* **1989**, *117*, 121.
(28) Mirodatos, C. *J. Phys. Chem.* **1986**, *90*, 481.
(29) Zhang, X.; Biloen, P. *J. Catal.* **1986**, *98*, 468.
(30) Mims, C. A.; McCandlish, L. E. *J. Am. Chem. Soc.* **1985**, *107*, 696.
(31) Mims, C. A.; McCandlish, L. E. *J. Phys. Chem.* **1987**, *91*, 929.
(32) Stockwell, D. M.; Bianchi, D.; Bennett, C. O. *J. Catal.* **1988**, *113*, 13.
(33) Sidall, J. H.; Miller, M. L.; Delgass, W. N. *Chem. Eng. Commun.* **1989**, *83*, 241.
(34) Vada, S.; Hoff, A.; Ådnanes, E.; Schanke, D.; Holmen, A. Fischer-Tropsch Synthesis on Supported Cobalt Catalysts Promoted by Platinum and Rhenium. Submitted to *J. Catal.*
(35) Vada, S.; Chen, B.; Goodwin, J. G., Jr. Isotopic Transient Study of La Promotion of Co/Al_2O_3 for CO Hydrogenation. Submitted to *J. Catal.*
(36) Vada, S.; Kazi, A. M.; Bedu-Addo, F. K.; Chen, B.; Goodwin, J. G., Jr. In *Natural Gas Conversion II*, Proceedings of the Third Natural Gas Conversion Symposium, Sydney, July 4–9, 1993; Curry-Hyde, H. E., Howe, R. F., Eds.; Elsevier Science Publishers: Amsterdam, 1994; Vol. 81, p 443.
(37) Zhang, X.; Biloen, P. *Chem. Eng. Commun.* **1986**, *44*, 303.
(38) Mims, C. A. *Catal. Lett.* **1988**, *1*, 293.
(39) Ali S.; Chen, B.; Goodwin, J. G., Jr. Zr Promotion of Co/SiO_2 for Fischer-Tropsch Synthesis. Submitted to *J. Catal.*
(40) Yang, C. H.; Soong, Y.; Biloen, P. In *Proceedings, 8th International Congress on Catalysis*, Berlin (West), 2–6 July, 1984; Verlag Chemie: Weinheim, West Germany, 1984; Vol. 2, p 3.
(41) Soong, Y.; Biloen, P. *Langmuir* **1985**, *1*, 768.
(42) Nwalor, J. U.; Hoost, T. E.; Godbole, G. G.; Goodwin, J. G., Jr.; Biloen, P. In *Proceedings, 9th International Congress on Catalysis*, Calgary, 1988; Phillips, M. J., Ternan, M., Eds.; Chemical Institute of Canada: Ottawa, ON, 1988; Vol. 2, p 875.
(43) Happel, J.; Suzuki, J.; Kokayeff, P.; Fthenakis, V. *J. Catal.* **1980**, *65*, 59.
(44) Happel, J.; Cheh, H. Y.; Otarod, M.; Ozawa, S.; Severdia, A. J.; Yoshida, T.; Fthenakis, V. *J. Catal.* **1982**, *75*, 314.
(45) Otarod, M.; Ozawa, S.; Yin, F.; Chew, M.; Cheh, H. Y.; Happel, J. *J. Catal.* **1983**, *84*, 156.
(46) Happel, J.; Cheh, H. Y.; Otarod, M.; Bajars, L.; Hnatow, M. A.; Yin, F. In *Proceedings, 8th International Congress on Catalysis*, Berlin (West), 2–6 July, 1984; Verlag Chemie: Weinheim, West Germany, 1984; Vol. 3, p 395.
(47) Yang, C. H.; Soong, Y.; Biloen, P. *J. Catal.* **1985**, *94*, 306.
(48) Mims, C. A.; McCandlish, L. E.; Melchior, M. T. *Catal. Lett.* **1988**, *1*, 121.
(49) Mims, C. A.; Krajewski, J. J.; Rose, K. D.; Melchior, M. T. *Catal. Lett.* **1990**, *7*, 119.
(50) Bell, A. T.; Winslow, P. In *Proceedings, 8th International Congress on Catalysis*, Berlin (West), 2–6 July, 1984; Verlag Chemie: Weinheim, West Germany, 1984; Vol. 3, p 175.
(51) Winslow, P.; Bell, A. T. *J. Catal.* **1984**, *86*, 158.
(52) Bell, A. T. In *Proceedings, 9th International Congress on Catalysis, Calgary, 1988*; Phillips, M. J., Ternan, M., Eds.; Chemical Institute of Canada: Ottawa, ON, 1988; Vol. 5, p 134.
(53) Hoost, T. E.; Goodwin, J. G., Jr. *J. Catal.* **1992**, *137*, 22.
(54) Krishna, K. R.; Bell, A. T. *Catal. Lett.* **1992**, *14*, 305.
(55) Krishna, K. R.; Bell, A. T. In *New Frontiers in Catalysis*, Proceedings of the 10th International Congress on Catalysis, Budapest, 19–24 July, 1992; Guczi, L., Solymosi, F., Tétényi, P., Eds.; Akadémiai Kiadó: Budapest, Hungary, 1993; Part A, p 181.
(56) Efstathiou, A. M. *J. Mol. Catal.* **1991**, *67*, 229.
(57) Efstathiou, A. M.; Bennett, C. O. *Chem. Eng. Commun.* **1989**, *83*, 129.
(58) Efstathiou, A. M.; Bennett, C. O. *J. Catal.* **1989**, *120*, 137.
(59) Efstathiou, A. M.; Chafik, T.; Bianchi, D.; Bennett, C. O. *J. Catal.* **1994**, *148*, 224.
(60) Koerts, T.; Welters, W. J. J.; van Santen, R. A. *J. Catal.* **1992**, *134*, 1.
(61) Koerts, T.; van Santen, R. A. *J. Catal.* **1992**, *134*, 13.
(62) Chuang, S. C.; Balakos, M. W.; Krishnamurthy, R.; Srinivas, G. In *Natural Gas Conversion II*, Proceedings of the Third Natural Gas Conversion Symposium, Sydney, July 4–9, 1993; Curry-Hyde, H. E., Howe, R. F., Eds.; Elsevier Science Publishers: Amsterdam, 1994; Vol. 81.
(63) Nwalor, J. U.; Goodwin, J. G., Jr. In Perspectives in Catalysis: Ammonia Synthesis and Beyond. Topsøe, H., Boudart, M., Norskøv, J. K., Eds. *Top. Catal.* **1994**, *1*.
(64) Ozkan, U. S.; Cai, Y.; Kumthekar, M. W. *J. Catal.* **1994**, *149*, 375.
(65) Ozkan, U. S.; Cai, Y.; Kumthekar, M. W. *J. Catal.* **1994**, *149*, 390.
(66) Haddad, G. J.; Goodwin, J. G., Jr. The Impact of Aqueous Impregnation on the Properties of Prereduced vs. Precalcined Co/SiO_2. Submitted to *J. Catal.*
(67) Vada, S.; Goodwin, J. G., Jr. Analysis of Li Promotion of Methanol Synthesis on Pd/SiO_2 using Isotopic Transient Kinetics. Submitted to *J. Phys. Chem.*
(68) Kazi, A. M.; Chen, B.; Goodwin, J. G., Jr.; Marcelin, G. Li^+ Promotion of Pd/SiO_2: The Effect on Hydrogenation, Hydrogenolysis, and Methanol Synthesis. Submitted to *J. Catal.*
(69) Lacombe, S.; Sanchez, J. G.; Delichere, P.; Mozzanega, H.; Tatibouet, J. M.; Mirodatos, C. *Catal. Today* **1992**, *13*, 273.
(70) Mirodatos, C.; Dalmon, J. A.; Martin, G. A. *J. Catal.* **1987**, *105*, 405.
(71) Mirodatos, C.; Holmen, A.; Mariscal, R.; Martin, G. A. *Catal. Today* **1990**, *6*, 601.
(72) Peil, K. P.; Goodwin, J. G., Jr.; Marcelin, G. *J. Catal.* **1991**, *131*, 143.
(73) Peil, K. P.; Marcelin, G. M.; Goodwin, J. G., Jr. In *Direct Methane Conversion by Oxidative Processes: Fundamental and Engineering Aspects*; Wolf, E. E., Ed.; Van Nostrand Reinhold: New York, 1992; p 138.
(74) Peil, K. P.; Goodwin, J. G., Jr.; Marcelin, G. *J. Phys. Chem.* **1989**, *93*, 5977.
(75) Peil, K. P.; Goodwin, J. G., Jr.; Marcelin, G. In *Natural Gas Conversion*, Proceedings of the Natural Gas Conversion Symposium, Oslo, August 12–17, 1990; Holmen, A., Jens, K.-J., Kolboe, S., Eds.; Elsevier Science Publishers: Amsterdam, 1991; Vol. 61, p 73.
(76) Efstathiou, A. M.; Lacombe, S.; Mirodatos, C.; Verykios, X. E. *J. Catal.* **1994**, *148*, 639.
(77) Kalenik, Z.; Wolf, E. E. *Catal. Lett.* **1991**, *9*, 441.
(78) Peil, K. P.; Goodwin, J. G., Jr.; Marcelin, G. *J. Am. Chem. Soc.* **1990**, *112*, 6129.
(79) Peil, K. P.; Goodwin, J. G., Jr.; Marcelin, G. *J. Catal.* **1991**, *132*, 556.

(80) Koranne, M. M.; Goodwin, J. G., Jr.; Marcelin, G. *J. Catal.* **1994**, *148*, 378.
(81) Koranne, M. M.; Goodwin, J. G., Jr.; Marcelin, G. *J. Phys. Chem.* **1993**, *97*, 673.
(82) Koranne, M. M.; Goodwin, J. G., Jr.; Marcelin, G. In *New Frontiers in Catalysis*, Proceedings of the 10th International Congress on Catalysis, Budapest, 19–24 July, 1992; Guczi, L., Solymosi, F., Tétényi, P., Eds.; Akadémiai Kiadó: Budapest, Hungary, 1993; Part A, p 119.
(83) Smith, M. R.; Ozkan, U. S. *J. Catal.* **1993**, *142*, 226.
(84) Mauti, R.; Mims, C. A. *Catal. Lett.* **1993**, *21*, 201.
(85) Ekstrom, A.; Lapszewicz, J. A. *J. Phys. Chem.* **1989**, *93*, 5230.
(86) Ekstrom, A.; Lapszewicz, J. A. *J. Am. Chem. Soc.* **1988**, *110*, 5226.
(87) Ekstrom, A.; Lapszewicz, J. A. *J. Chem. Soc., Chem. Commun.* **1988**, 797.
(88) Ekstrom, A.; Lapszewicz, J. A. *Symposium on Direct Conversion of Methane to Higher Homologues*, American Chemical Society Los Angeles Meeting, Sept. 25–30, 1988; The Division of Petroleum Chemistry, Inc., American Chemical Society: Washington, DC, 1988; p 430.
(89) Oukaci, R.; Blackmond, D. G.; Goodwin, J. G., Jr.; Gallaher, G. R. In *Catalytic Control of Air Pollution: Mobile and Stationary Sources*; Silver, R. G., Sawyer, J. E., Summers, J. C., Eds.; ACS Symposium Series 495; American Chemical Society: Washington, DC, 1992; Chapter 5, p 61.
(90) Saleh-Alhamed, Y. A.; Hudgins, R. R.; Silveston, P. L.; Peil, K. P.; Goodwin, J. G., Jr. Unpublished work at the University of Pittsburgh, Pittsburgh, PA, 1992.
(91) Bariås, O. A. Ph.D. Dissertation, University of Trondheim, Trondheim, Norway, 1993.
(92) Happel, J.; Kao, J.-Y.; Yoshikiyo, M.; Chen, Z.; Takeyasu, O.; Hnatow, M. A.; Cheh, H. Y.; Walter, E.; Lecourtier, Y. In *Proceedings, 9th International Congress on Catalysis, Calgary, 1988*; Phillips, M. J., Ternan, M., Eds.; Chemical Institute of Canada: Ottawa, ON, 1988; p 1457.
(93) Kao, J.-Y.; Piet-Lahanier, H.; Walter, E.; Happel, J. *J. Catal.* **1992**, *133*, 383.
(94) Crathorne, E. A.; MacGowan, D.; Morris, S. R.; Rawlinson, A. P. *J. Catal.* **1994**, *149*, 254.
(95) Balakos, M. W.; Chuang, S. S. C. *J. Catal.* **1995**, *151*, 253.
(96) Balakos, M. W.; Chuang, S. S. C. *J. Catal.* **1995**, *151*, 266.
(97) Hoost, T. E.; Goodwin, J. G., Jr. In *Catalyst Deactivation 1991*; Bartholomew, C. H., Butt, J. B., Eds.; Elsevier Science Publishers: Amsterdam, 1991; p 691.
(98) Russell, A. J.; Chatterjee, S.; Rapanovitch, I.; Goodwin, J. G., Jr. In *Biomolecules in Organic Solvents*; CRC Press: West Palm Beach, FL, 1992; p 91.

CR940051C